SEA BREEZE: STRUCTURE, FORECASTING, AND IMPACTS

S. T. K. Miller,[1] B. D. Keim,[2,3] R. W. Talbot,[1] and H. Mao[1]
Climate Change Research Center, Institute for the Study of Earth, Oceans and Space, University of New Hampshire, Durham, New Hampshire, USA

Received 15 January 2003; revised 9 June 2003; accepted 19 June 2003; published 16 September 2003.

[1] The sea breeze system (SBS) occurs at coastal locations throughout the world and consists of many spatially and temporally nested phenomena. Cool marine air propagates inland when a cross-shore mesoscale (2–2000 km) pressure gradient is created by daytime differential heating. The circulation is also characterized by rising currents at the sea breeze front and diffuse sinking currents well out to sea and is usually closed by seaward flow aloft. Coastal impacts include relief from oppressive hot weather, development of thunderstorms, and changes in air quality. This paper provides a review of SBS research extending back 2500 years but focuses primarily on recent discoveries. We address SBS forcing mechanisms, structure and related phenomena, life cycle, forecasting, and impacts on air quality.
INDEX TERMS: 3329 Meteorology and Atmospheric Dynamics: Mesoscale meteorology; 3307 Meteorology and Atmospheric Dynamics: Boundary layer processes; 3322 Meteorology and Atmospheric Dynamics: Land/atmosphere interactions; 3339 Meteorology and Atmospheric Dynamics: Ocean/atmosphere interactions (0312, 4504); 3399 Meteorology and Atmospheric Dynamics: General or miscellaneous; *KEYWORDS:* sea breeze
Citation: Miller, S. T. K., B. D. Keim, R. W. Talbot, and H. Mao, Sea breeze: Structure, forecasting, and impacts, *Rev. Geophys., 41*(3), 1011, doi:10.1029/2003RG000124, 2003.

1. INTRODUCTION

[2] The sea breeze is a local *circulation* that occurs at coastal locations throughout the world [*Masselink and Pattiaratchi*, 1998]. (Italicized terms are defined in the glossary, after the main text.) It has been observed from polar regions to the equator. The sea breeze can provide relief from oppressive hot weather, trigger thunderstorms, provide moisture for fog and may result in either improved or reduced air quality near Earth's surface [*Barbato*, 1975; *Kozo*, 1982; *Hsu*, 1988; *Simpson*, 1994; *Camberlin and Planchon*, 1997; *Silva Dias and Machado*, 1997]. It is important to continue improving our understanding of the sea breeze because a large part of the human population lives in major cities in coastal areas.

[3] The large-scale environment in which the sea breeze occurs has been understood for thousands of years, and the broad outlines of the sea breeze's behavior have been understood for at least a hundred years. It occurs under relatively cloud-free skies, when the surface of the land heats up more rapidly than the sea. The thermal contrast creates a local-scale *pressure gradient force* (PGF) directed from sea to land, and a shallow layer of marine air moves inland in response. Some of the components of the *sea breeze system* (SBS) (Figure 1) are the following:

1. Sea breeze circulation (SBC) is a vertically rotating *mesoscale* cell, with shoreward flow near Earth's surface, rising air currents inland, diffuse sinking currents several kilometers out to sea, and (usually) seaward return flow near 900 *hPa*.
2. *Sea breeze gravity current* (SBG) is the landward flow of cool, moist marine air in the lower horizontal arm of the SBC.
3. *Sea breeze front* (SBF) is the landward edge of the SBG and the SBC, often associated with sharp changes in temperature, moisture, and wind. Its approach may be marked by the development of fair-weather cumulus clouds (*Cu*).
4. *Sea breeze head* (SBH) is the raised head above and immediately behind the SBF, created by updrafts within both the continental and marine air masses. It is about twice as high as the following "feeder" flow behind the SBF.
5. *Kelvin-Helmholtz billows* (KHBs) are waves that develop along the upper boundary of the SBG during periods of low static stability (midday).
6. *Convective internal boundary layer* (CIBL) is an unstable region within the marine air mass, appearing at the coast and growing in depth with distance inland, in which low-level pollutants may become trapped and concentrated.

[1]Also at Department of Earth Sciences, University of New Hampshire, Durham, New Hampshire, USA.
[2]Also at Department of Geography, University of New Hampshire, Durham, New Hampshire, USA.
[3]Now at Southern Regional Climate Center, Louisiana State University, Baton Rouge, Louisiana, USA.

8755-1209/03/2003RG000124*$15.00* doi:10.1029/2003RG000124

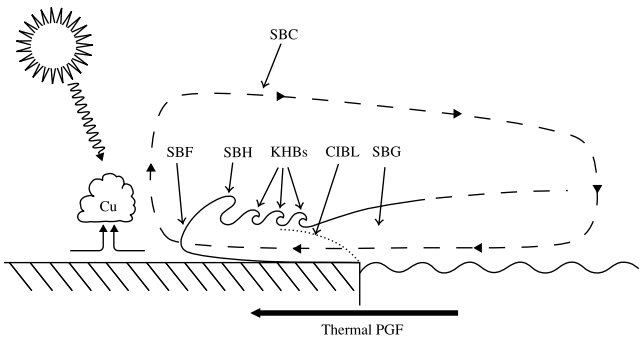

Figure 1. Sea breeze system (SBS). Details are discussed in the text.

[4] The details of the sea breeze's behavior along specific coastlines can be surprising, even to experienced meteorologists. For example, while the sea breeze is initiated during the daytime, it may persist at any time during the day or night. The leading edge of the sea breeze may separate from the feeder flow behind the front and move hundreds of kilometers inland as an independent entity.

[5] A great deal of new knowledge has been gained over the last 15 years, and an updated overview is needed, tying together our improved understanding of the sea breeze. This paper will fill that need, focusing on sea breeze forcing mechanisms, structure, life cycle, forecasting, and the ways in which the sea breeze impacts local air quality. The glossary contains key terms, and the notation list defines symbols used in this paper.

2. ANCIENT HISTORY

[6] Given their dependence on the wind and tides, it seems likely that early sailors and fishermen understood the diurnal cycle of the sea breeze long before natural scientists began writing about it. Military personnel, particularly those that fought battles at sea, would also have been keenly interested in the sea breeze. *Simpson* [1994] discusses the story of Athenian military leader Themistocles, commander of the Greek forces in a naval battle with the Persians in 480 B.C. The battle took place in a narrow channel between the island of Salamis and the Greek mainland. Themistocles chose to begin his battle with the Persians at the moment when the sea breeze began flowing into the narrow channel. The low, solid design of the Greek ships gave them the advantage in the choppy waters caused by the sea breeze, and they defeated the Persians.

[7] The first scientist to write about the wind in general was Aristotle. In *Meteorologica*, written 150 years after Themistocles' victory at Salamis, Aristotle stated that "as a rule a considerable area may be expected to be similarly affected, because neighboring places lie in a similar relation to the Sun, unless they have some local peculiarity" (as quoted by *Lee* [1952, p. 169]). He noted that the *prevailing wind* in Athens is from the north or south, and the Etesian wind, a persistent, northerly or northeasterly wind, occurs after the summer solstice. Aristotle attributed local-scale winds to the unequal distribution of Earth's moist and dry "exhalations" and variations in local topography [*Lee*, 1952, p. 165].

[8] Theophratus' *De Ventis* was written about 300 B.C., ~30 years after *Meteorologica*, and discusses (1) the importance of the Sun in driving the wind and (2) a distinct sea breeze from the south or southwest that occurred during the period of the Etesian wind. According to Theophratus, "at about the time of the Etesians, winds arise counter to the north wind because of a circling back so that ships move in the opposite direction. These winds are called reverse north winds" (as quoted by *Coutant and Eichenlaub* [1975, p. 29]). This may be the first written reference to an onshore wind opposing a synoptic (continental)-scale offshore wind. Theophratus also noticed that "everywhere at noon the winds die down because of the Sun's actions, and arise again with the late afternoon. It happens that the reversing wind [the seabreeze] blows against the land winds and the Etesians rise at the same time again" [*Coutant and Eichenlaub*, 1975, p. 31]. This observation can be explained as opposing forces reaching equilibrium at about noontime, and Theophratus correctly attributed the developing equilibrium to the Sun's influence. During midafternoon, when the land-sea temperature contrast reaches its maximum, the sea breeze moves inland as a southwesterly wind, while well offshore the northeasterly Etesian wind reaches its diurnal maximum [*Coutant and Eichenlaub*, 1975].

[9] As far as we know, there is little documented to demonstrate major advances in the understanding of the sea breeze from about 300 B.C. to the seventeenth century A.D. This gap in research is a subject best addressed by historians. Over the past several centuries, there has been an increasing interest in the sea breeze, which is documented in *Jehn*'s [1973] bibliography of sea breeze research from the seventeenth century to 1972. He lists 16 references on the sea breeze written before 1800, 113 written between 1800 and 1899, and 407 written between 1900 and 1972. Among Jehn's references are a brief article by Francis Bacon, written in 1664, and another by Immanuel Kant from 1755 [*Jehn*, 1973]. A recent search reveals more than 500 new articles published on the subject since 1990 alone.

3. MODERN UNDERSTANDING

[10] Contemporary studies of the sea breeze system have been motivated by its influence on local wind velocity and air quality [e.g., *Angell and Pack*, 1965; *Yu and Wagner*, 1970; *Barbato*, 1975; *Neumann*, 1977; *Shair et al*., 1982; *Kalthoff et al*., 2002] and convective activity [e.g., *Pielke*, 1985; *Pielke et al*., 1991; *Rao and Fuelberg*, 2000; *Lericos et al*., 2002], as well as by an interest in the

Table 1. Summary of Subjects Discussed in Sea Breeze Literature

General Subject	*Specific Topics Included*
Forcing	the role of sound waves; development of the sea breeze circulation from the mesoscale pressure gradient; more complete physical models
Structure	prefrontal phenomena; sea breeze's response to the prevailing wind; sea breeze gravity current and its response to Kelvin-Helmholtz billows; sea breeze front and associated phenomena
Life cycle	sequence of development stages
Interactions with external meteorological phenomena	separate sea breeze systems; convective updrafts; urban heat islands; river breezes; temperature inversions; horizontal convective rolls; synoptic-scale cold fronts
Forecasting	occurrence of a sea breeze; wind speed and direction; extent of inland penetration
SBS-related air quality impact mechanisms	pollutant transport mechanisms; convective internal boundary layers; sea breeze in complex air pollution scenarios

more esoteric aspects of its dynamics and structure [e.g., *Smith*, 1982; *Kraus*, 1992; *Reible et al*., 1993; *Tijm and van Delden*, 1999]. Some have even studied SBS influence on the coastal ocean [*Schoellhamer*, 1996; *Gibbs*, 2000] and beach morphology [*Masselink and Pattiaratchi*, 1998].

[11] These researchers have found that the SBS, often thought to be easily understood, is actually a very complicated phenomenon, producing associated phenomena or nonlinear interactions on several scales, from the meso-β scale (20–200 km) through the inertial subrange (where turbulent motions are approximately homogeneous, *isotropic*, and *inviscid*) [*Stull*, 1988; *Finkele et al*., 1995; *Cenedese et al*., 2000]. Some of the phenomena are the raised head of the advancing sea breeze [e.g., *Craig et al*., 1945; *Simpson*, 1994]; interactions between the sea breeze or sea breeze front and *synoptic-scale* or other mesoscale circulations [e.g., *Zhong and Takle*, 1992; *Atkins et al*., 1995; *Brümmer et al.*, 1995], as well as between multiple sea breeze fronts [*Clarke*, 1984]; the turbulent wake composed of Kelvin-Helmholtz billows seaward of the sea breeze front and along the upper boundary of the shallow marine layer [e.g., *Chiba et al*., 1999]; and the CIBL that forms within the stable marine layer as it moves over the hot land surface [e.g., *Hsu*, 1988].

[12] In sections 3.1–3.6 each of the areas summarized in Table 1 will be explored in detail.

3.1. Forcing

3.1.1. Role of Sound Waves

[13] The sea breeze is caused by the temperature difference between the hot land and cool sea surfaces. As the difference increases during the day, a pressure gradient is produced at low levels in the atmosphere, initiating the sea breeze near Earth's surface [*Simpson*, 1994]. The appearance of the *mesoscale pressure gradient force* (PGF) that drives the SBS may seem relatively simple to explain, but *Tijm and van Delden* [1999] carefully examined three different variations found in the literature and concluded that all three are physically inconsistent.

[14] The first is the "upward" theory [*Tijm and van Delden*, 1999], wherein a seaward flow (sometimes called return flow) develops aloft first, because of the vertical expansion of the warmer air over land. Landward flow near Earth's surface then develops in response to the seaward flow aloft. The second is called the "sideways" theory [*Simpson*, 1994], wherein the low-level onshore flow develops first in response to the horizontal expansion of the warmer air over land. Seaward (return) flow aloft then develops in response to the low-level onshore flow. The third is called the "mixed" theory [*Godske et al*., 1957], in which the warmer air over land expands both vertically and horizontally, causing the simultaneous development of the surface sea breeze and the return current aloft [*Tijm and van Delden*, 1999].

[15] All three versions, in spite of some evidence in the synoptic surface observations to support them, neglect the process of *hydrostatic* adjustment. This occurs in the developing SBS and is accompanied by the creation of sound (compression) waves, which are generated over land when the air expands because of *diabatic* heating and then propagate at 300 m s^{-1} in all directions [*Tijm and van Delden*, 1999]. Utilizing a nonhydrostatic computer model, *Tijm and van Delden* [1999] concluded that sound waves play a critical role in establishing the mesoscale pressure gradient. *Walsh* [1974] concluded earlier that simulations of the sea breeze circulations using nonhydrostatic models differ very little from those produced by hydrostatic models, but the *Tijm and van Delden* [1999] results indicate that the small difference between the two model schemes is important, because the hydrostratic models do not incorporate sound waves and therefore do not include the correct mechanism for establishing the mesoscale pressure gradient.

[16] Within a few minutes, sound waves traveling upward induce an increase in pressure through the entire atmosphere above the heated land surface. Waves propagating horizontally induce pressure falls over land, and surface pressure increases over the sea. The resulting horizontal pressure gradient initiates the landward movement of the marine air mass associated with the

SBS. The surface pressure decrease over land is first seen at the coast, but locations more than 1000 km inland experience a decline in pressure within an hour. These results are supported by a careful analysis of the synoptic surface record in Europe and represent a more physically consistent version of the mixed theory [*Tijm and van Delden*, 1999].

3.1.2. Sea Breeze Circulation (SBC) and the Bjerknes Circulation Theorem

[17] Mathematical models, when used in conjunction with field observations, are a powerful means for exploring physical mechanisms. The Bjerknes circulation theorem is a relatively simple model that begins with the presence of a cross-shore mesoscale PGF and reproduces the SBC from an initially stationary atmosphere. Circulation is a scalar quantity that represents a macroscopic measure of rotation over a finite area of fluid in two dimensions [*Holton*, 1992]. Mathematically, circulation about a closed contour in a fluid is defined as the line integral about the contour of the component of the velocity vector that is locally tangent to the contour [*Holton*, 1992]. The Bjerknes circulation theorem is given by

$$\frac{D_a C_a}{Dt} = -\oint \frac{dP}{\rho}, \tag{1}$$

where D_a/D_t indicates the material derivative in the fixed reference frame, C_a is circulation, P is pressure [Pa], and ρ is density [kg m^{-3}].

[18] The application of the circulation theorem to the SBC begins with equation (1) and substitutes $\rho = P/RT$ (from the ideal gas law), where T is temperature [K] and R is the gas constant for dry air (287 J kg^{-1} K^{-1}). By integrating around the closed path beginning on the land surface (Figure 2, lower left) and using the fact that the line integral about a closed loop of a perfect differential is zero, one obtains

$$\frac{DC_a}{Dt} = R\ln\left(\frac{p_0}{p_1}\right)(\overline{T}2 - \overline{T}1), \tag{2}$$

where p_0 represents atmospheric pressure near Earth's surface [Pa], p_1 represents atmospheric pressure near the top of the circulation cell [Pa], and $\overline{T}$ indicates the average temperature through the vertical column [*Holton*, 1992].

[19] To extract the mean wind speed ($\overline{U}$) associated with the SBS, one uses

$$\overline{U} = \frac{C_a}{2(H + L)}, \tag{3}$$

where H is the height of the circulation and L is its cross-shore length (Figure 2). Combining equations (2) and (3) yields

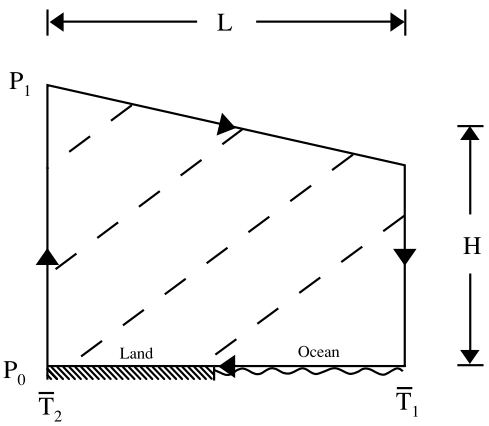

Figure 2. Sea breeze and the Bjerknes circulation theorem. Land is on the left, ocean is on the right. The integration path for equation (1) is indicated by arrows along the perimeter. $\overline{T}$ indicates the average temperature through the vertical columns over the land or ocean surfaces. Dashed diagonal lines are isopycnals, with denser air at lower right. P_0 and P_1 are the pressure on the surface and at the top of the circulation cell, respectively. Redrawn from *Holton* [1992]. Reprinted with permission from Elsevier Science.

$$\frac{D\overline{U}}{Dt} = \frac{R\ln\left(\frac{p_0}{p_1}\right)(\overline{T}2 - \overline{T}1)}{2(H + L)}, \tag{4}$$

which is an expression for the mean acceleration of the wind over time, as a result of the SBC. Realistic values for the right-hand side of equation (4) are p_0 = 1000 hPa, p_1 = 900 hPa, $(\overline{T}2 - \overline{T}1)$ = 10 K, L = 20 km, and H = 1 km, which yields an acceleration of 7.2 $\times 10^{-3}$ m s^{-2}. Beginning at rest, after 1 hour the mean wind speed around the perimeter is 25.9 m s^{-1} or ~50 knots [*Holton*, 1992].

[20] Wind speeds actually produced by the SBS are generally much lower than those suggested by the circulation theorem. *Simpson* [1994] suggested that surface wind speeds of 6 or 7 m s^{-1} can reasonably be expected. Other authors [e.g., *Masselink and Pattiaratchi*, 1998] have suggested that speeds as high as 10 m s^{-1} are common. The main reason for this overestimate is that in the initial formulation the Bjerknes circulation theorem assumes friction (in its various forms) is too small to be of importance. Another weakness of this application, perhaps just as important, is that it ignores the alongshore dimension.

3.1.3. More Complete Models and Topography

[21] The following factors affecting the SBS should be included in a complete physical model [*Simpson*, 1994]: (1) diurnal variation of the ground temperature, (2) *diffusion* of heat, (3) static stability, (4) *Coriolis force*(s), (5) diffusion of momentum, (6) topography, and (7) prevailing wind. The first two are essential for the sea breeze to occur, and the third is a factor in its inland movement [*Simpson*, 1994]. The Coriolis force, while

unimportant for the first 6 hours, is responsible for producing the horizontal rotation of the SBS over time and thus limits the extent of its inland penetration [*Pearce*, 1955; *Neumann*, 1977; *Anthes*, 1978; *Simpson*, 1996]. Momentum diffusion is important for producing the observed near-surface wind profile, is the most important brake on the developing circulation, and prevents the SBS from producing the very high wind speeds predicted by the Bjerknes circulation theorem [*Anthes*, 1978; *Simpson*, 1994]. SBS response to prevailing (synoptic-scale) wind is discussed in section 3.2.2.

[22] Topography, including the size and shape of the landmass and the details of the coastline, is another important factor in the SBS. Many early models investigating SBS behavior assumed straight coastlines and flat topography [e.g., *Estoque*, 1962] but included terms corresponding to the other six items listed. More recent authors discuss the behavior of the SBS in more realistic physical settings. Most of their conclusions are necessarily specific to the geographical region examined, although some important general conclusions are obtained.

3.1.3.1. Seaward Facing Slopes

[23] If a hill is located just inland of a flat coastal plain, with its slope facing the sea, the influence of the hill on the SBS is determined by the hill's surface temperature cycle. When the temperature of the slope varies with the same diurnal period as that of the coastal plain, the SBS is amplified and occurs earlier than it would if the hill were not present. If the slope acts as a barrier only (i.e., is enshrouded in fog or clouds), the SBS is confined to the coastal plain. *Asai and Mitsumoto* [1978] originally described this effect with a computer model, and *Banta et al*. [1993] observed it on the west coast of the United States using a pulsed Doppler lidar.

3.1.3.2. Bays

[24] When a bay is located on an otherwise straight, east-west coastline with the ocean to the south, the bay causes the sea breeze to bow landward relative to the straight sections of coastline on either side. Within the convergence zone between the sea breeze and the seaward synoptic-scale flow, there are regions of enhanced upward and downward vertical motion related to the position of the bay but distributed asymmetrically. In the Northern Hemisphere, enhanced convergence and vertical motion occur to the west of the bay, where the PGF and Coriolis force act in opposition to each other, and weakened convergence and vertical motion occur on the east side of the bay, where the two forces act in the same direction [*McPherson*, 1970].

3.1.3.3. Narrow Landmasses

[25] When two sea breeze systems form on opposite sides of a narrow landmass, the interactions that result when they converge at the center of the landmass are partially determined by the width of the landmass [*Xian and Pielke*, 1991]. The thermal forcing over a narrow peninsula or island (width $<$100 km) is insufficient for developing a deep, well-organized mesoscale circulation, and both sea breeze systems are weak. For landmasses with widths between 100 and 150 km the thermal forcing is strong enough to develop deep systems, and the landmass is still narrow enough so that the two opposite systems converge at the center and produce a region of deep *convection*. Landmasses $>$150 km across are too wide for the two opposing systems to reach each other before sunset, and the associated convergence region in the center of the landmass is weakened [*Xian and Pielke*, 1991]. When the two opposing sea breeze systems reach each other during the evening hours (when the ambient atmosphere is stable), undular bores may result [*Clarke*, 1984].

3.1.3.4. Complex Terrain

[26] Complex terrain, with or without nonzero synoptic-scale flow, may produce several separate sea breeze systems along different portions of the coastline. The appearance of these independent systems may not be simultaneous, and they may not ultimately reach the same intensities. Inland topographic features channel the low-level flow, creating areas of enhanced convergence and upward vertical motion. Upward vertical motion is also enhanced where different sea breeze systems converge at points inland [*Melas et al*., 1998, 2000].

3.1.3.5. Temperature Characteristics of Land and Sea Surfaces

[27] Stronger SBS-associated wind speeds occur with stronger cross-shore temperature gradients. *Schumann et al*. [1991] noted this effect in the sea breeze of Alcoa Bay, South Africa, where the strongest sea breeze occurs in areas with nearby dune fields. During the daytime the sand dunes create a region of superheated air immediately overhead, setting up a very strong land-sea temperature difference. *Coastal upwelling*, which brings colder water to the surface, also enhances the cross-shore temperature gradient. On the east coast of a continent in the Northern Hemisphere, *upwelling* (driven by *Ekman pumping*) occurs when there is an alongshore wind component, with low pressure to the west and high pressure to the east [*Apel*, 1987]. *Franchito et al*. [1998] observed that the SBS of coastal Brazil is stronger during periods of upwelling and weaker when there is no upwelling.

3.2. Structure

[28] The SBS consists of phenomena occurring on several spatial scales (Figure 1). A summary of these includes the initiating sound waves discussed by *Tijm and van Delden* [1999], the sea breeze forerunner and similar prefrontal waves [*Geisler and Bretherton*, 1969; *Sha et al*., 1993], the closed cell of circulation predicted by the Bjerknes circulation theorem [*Holton*, 1992], the sea breeze gravity current and all of its associated phe-

nomena [e.g., *Simpson*, 1997], the sea breeze front and all of its associated phenomena [e.g., *Kraus et al*., 1990; *Kraus*, 1992; *Reible et al*., 1993], and smaller-scale phenomena, such as a convective internal boundary layer, within the landward moving marine air mass [*Hsu*, 1988; *Zhong and Takle*, 1992; *Rao and Fuelberg*, 2000]. One must also include interactions between all of these phenomena and with phenomena originating from other processes in both the atmosphere and ocean [e.g., *Brümmer et al*., 1995; *Gibbs*, 2000].

3.2.1. Prefrontal Phenomena

[29] In addition to the sound waves that initiate the cross-shore mesoscale PGF, another type of transitory wave precedes the arrival of the sea breeze front on land. The sea breeze forerunner is actually a cluster of waves that is initiated when the cross-shore thermal contrast appears above the land-sea interface. The waves with the largest amplitude arrive at points inland first, moving at speeds much faster than the sea breeze front. Over time, progressively smaller-scale waves arrive inland. Observers on Earth's surface will experience a wind from the direction of the sea consisting of local (continental) air before the arrival of the sea breeze front. The model results from *Geisler and Bretherton* [1969] indicate that with reasonable values of internal (eddy) viscosity and surface friction the forerunner reaches as far inland as 60 km.

[30] Another type of prefrontal wave may occur in the late evening, when the sea breeze front interacts with an inland *nocturnal stable layer*. These waves consist of small overturning cells with a characteristic wavelength of ~10 km, propagate inland at approximately 3.5 m s^{-1}, and rapidly dissipate in the ambient flow field [*Sha et al*., 1993].

3.2.2. SBC Response to the Synoptic-Scale Wind

[31] The SBC begins when a landward component is added to the net low-level wind vector in response to the mesoscale thermal PGF, resulting in a divergence in the cross-shore wind component over the sea. The shore-parallel zone in which the new wind component is added grows horizontally in the cross-shore direction, expanding more rapidly seaward than landward [*Finkele et al*., 1995]. A shallow layer of marine air begins flowing toward the land, converging with continental air and creating a region of upward vertical air currents (Figure 1).

[32] A seaward return flow usually develops aloft, above the upper boundary of the marine air, creating a shear zone where the flow changes directions from landward to seaward [*Finkele et al*., 1995; *Camberlin and Planchon*, 1997; *Tijm et al*., 1999; *Oliphant et al*., 2001]. This return flow is required if the SBC is to be considered closed, i.e., mass conservative. Several authors, however, report either the complete absence of this return flow or its insufficiency at counterbalancing the low-level onshore flow, implying that the SBC may not be a closed system under some circumstances [*Estoque*, 1962; *Intrieri et al*., 1990; *Banta et al*., 1993]. The upper limit of the circulation varies from a few hundred meters to 1 or 2 km, depending on synoptic conditions [*Frizzola and Fisher*, 1963; *Barbato*, 1975; *Intrieri et al*., 1990; *Xian and Pielke*, 1991]. On the other hand, *Tijm et al*. [1999] found that the seaward return flow may overcompensate for the low-level landward flow by as much as 30% (with respect to mass), creating a landward "return-return" flow above ~4 km. Weak sinking currents have been observed in situ and in model results over a broad area several tens of kilometers offshore, supporting a closed SBC with at least partial mass conservation [*Estoque*, 1962; *Neumann and Mahrer*, 1971; *Elliott and O'Brien*, 1977; *Asimakopoulos et al*., 1999; *Chiba et al*., 1999].

[33] The prevailing wind (PW) plays a large role in determining the shape and shore-relative location of the SBC. The PW is important in determining whether or not a sea breeze will be detectable on land (a very strong offshore PW will prevent the SBC from reaching the coast), as well as exerting an influence on its behavior [e.g., *Finkele et al*., 1995]. *Mizuma*'s [1995, 1998] observational studies of SBC behavior on the coast of Japan include descriptions of several manually identified sea breeze modes, which are dependent on the shape of the local coastline and the direction and strength of the PW. Several other studies have examined SBC response to the PW both generically and along specific coastlines [e.g., *Fisher*, 1960; *Estoque*, 1962; *Pearson et al*., 1983; *McKendry and Roulet*, 1994; *Planchon and Cautenet*, 1997; *Melas et al*., 1998; *Asimakopoulos et al*., 1999; *Clappier et al*., 2000; *Melas et al*., 2000; *Laird and Kristovich*, 2001; *Oliphant et al*., 2001; *Lericos et al*., 2002].

3.2.2.1. Generic Categories of Sea Breeze Circulation

[34] The SBC falls into four PW-dependent categories: pure, corkscrew, backdoor, and synoptic [*Adams*, 1997]. The fourth stretches the definition of the sea breeze from a locally driven circulation to any wind blowing from sea to land, and therefore this category will not be addressed here. The remaining three are described below in the context of the east coast of a Northern Hemisphere continent.

[35] A pure sea breeze [*Adams*, 1997] occurs under light PW conditions, when the existing geostrophic forcing points seaward at a right angle to the coastline, and closely matches the general description given above (Figures 3a–3c). This type of sea breeze is preceded by calm conditions, when the synoptic-scale PGF is briefly in equilibrium with the locally created thermal PGF. *Ohashi and Kida* [2001] noted its presence in Japan, ahead of an advancing SBG and below 800 m above ground level (AGL). *Chiba et al*. [1999], using an instrumented helicopter, observed that the calm region extends to ~10 km offshore. The SBC expands throughout the day, with the landward extreme reaching as far inland as ~130 km [*Adams*, 1997].

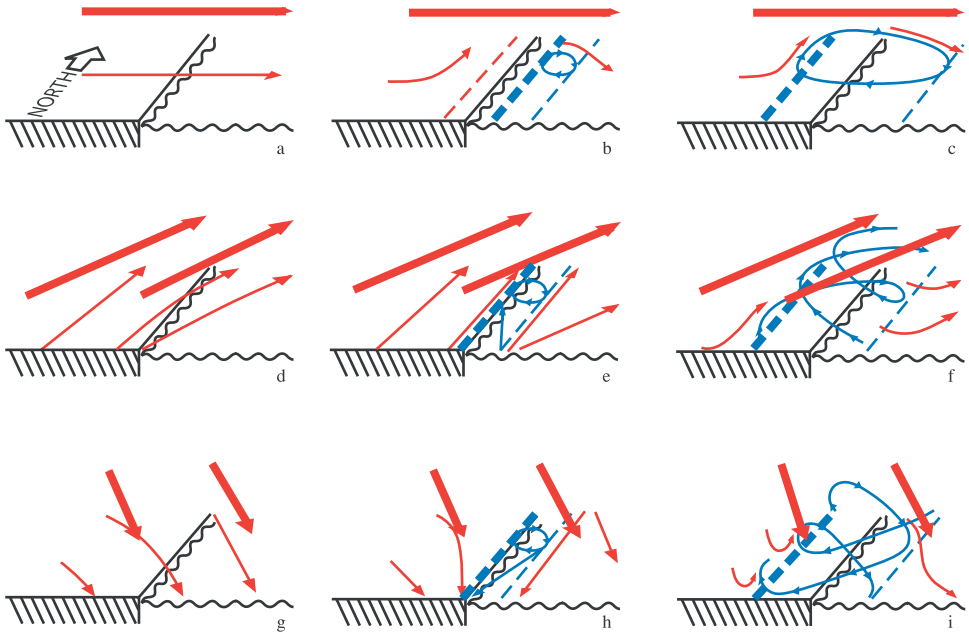

Figure 3. Development of pure, corkscrew, and backdoor sea breezes. Land is on the left; ocean is on the right. North is into the page. Bold red arrows indicate wind at the top of the planetary boundary layer. Thin red arrows indicate near-surface wind not related to sea breeze circulation (SBC). Blue arrows indicated SBC-related near-surface wind. Bold dashed blue line indicates inland limit of SBC; thin dashed blue line indicates seaward extent. (a, b, and c) Development of pure sea breeze. Dashed red line indicates inland extend of calm region that extends offshore to the first dashed blue line. (d, e, and f) Development of corkscrew sea breeze. (g, h, and i) Development of backdoor sea breeze. After *Adams* [1997].

[36] The corkscrew sea breeze [*Adams*, 1997] occurs when the PW has both along-shore and cross-shore components (Figures 3d–3f). The along-shore component is northward on the east coast of the hypothetical Northern Hemisphere landmass. According to *Buys-Ballot's law*, a northward wind component implies lower pressure over land and higher pressure over water [*Lutgens and Tarbuck*, 2001]. When differences in the coefficient of surface friction are taken into account, a northward wind component and lower pressure over land imply an area of low-level divergence near the coast. Air from aloft sinks into the divergence zone and assists with the initiation of the sea breeze. Since the thermal PGF and the synoptic-scale PGF are not entirely oriented along the same dimension, the former does not have to overcome the full magnitude of the latter, and therefore there is no calm period prior to the onset of the sea breeze. This also implies that a corkscrew sea breeze can reach the coast with a weaker thermal PGF, relative to a pure sea breeze. The arrival of the corkscrew sea breeze is marked by a gradual *backing* (rotation in the counterclockwise direction) of the wind from southwest to southeast. Like the pure sea breeze, the corkscrew sea breeze circulates in a vertical cell, but the along-shore component of the synoptic wind causes the circulation to take on a helical shape rather than a simple loop [*Adams*, 1997].

[37] The backdoor sea breeze [*Adams*, 1997] also occurs when the PW has along-shore and cross-shore components (Figures 3g–3i). In this case the along-shore component is southward on the east coast of the hypothetical Northern Hemisphere landmass. Buys-Ballot's law implies that lower pressure is over the ocean, and higher pressure is over the land [*Lutgens and Tarbuck*, 2001]. This, combined with the cross-shore variation in the coefficient of surface friction, results in an area of low-level convergence near the coast. This surface convergence prevents air from sinking from aloft and inhibits the sea breeze's progress toward land. This also implies that a backdoor sea breeze can only reach the coast with a stronger thermal PGF, relative to a pure or corkscrew sea breeze. As with the corkscrew sea breeze, arrival of a backdoor sea breeze is marked by a gradual shift in wind direction from northwest to northeast. In this case the wind veers (rotates in a clockwise direction) rather than backs. The backdoor sea breeze also rotates helically rather than in a simple loop, although in this case the along-shore *geostrophic wind* component causes the helix to spiral southward rather than northward. The other important differences between the corkscrew and backdoor sea breezes are that the latter is much weaker, arrives on land later in the day, and may manifest in pulses rather than strong, steady flow [*Adams*, 1997].

3.2.2.2. Examples of Sea Breeze Circulation

[38] A series of case studies carried out on the coast of New England provide real-world comparisons to the idealized sea breeze scenarios described in section

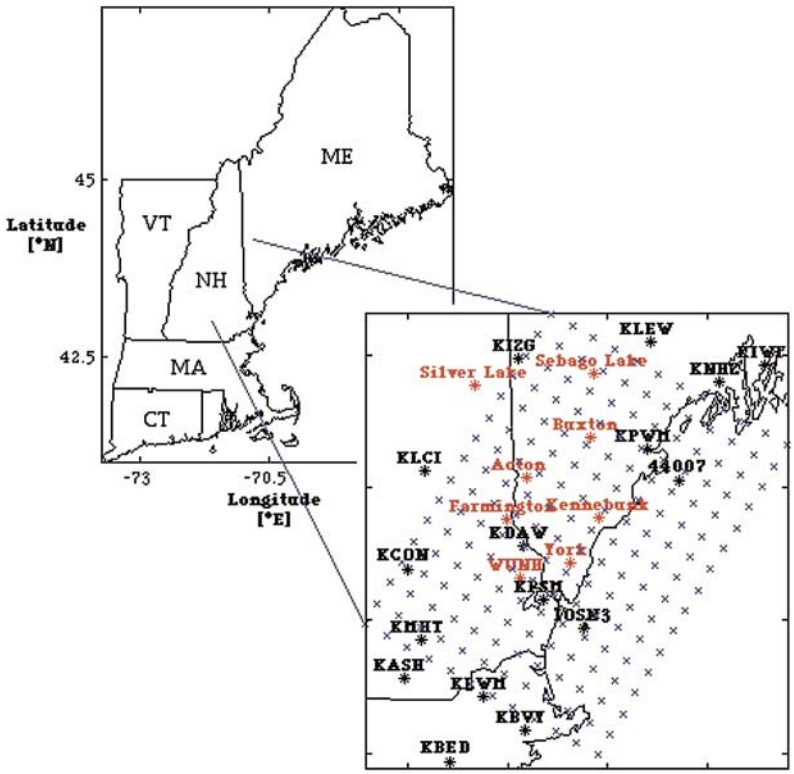

Figure 4. New England Air Quality Study, 2002, sea breeze study area. The sea breeze was closely studied along the relatively straight section of coastline from Lawrence, Massachusetts (KLWM), through north of Portland, Maine (KPWM) (see inset, lower right). Standard National Oceanic and Atmospheric Administration surface weather observing sites are labeled in black lettering with their International Civil Aviation Organization Identifiers. Stations added by the University of New Hampshire to improve the spatial resolution are shown in red. Data from all stations were combined and interpolated onto the 10-km rectangular grid shown in blue.

3.2.2.1. The study area shown in Figure 4 is nearly ideal for comparison to the hypothetical sea breezes shown in Figure 3, because the central 90% of the coastline is reasonably straight and can be approximated by a straight line rotated 30° clockwise from true north. These sea breeze events were observed during the *New England Air Quality Study* (NEAQS) 2002 summer campaign, which involved researchers from the U.S. National Oceanic and Atmospheric Administration (NOAA), the University of New Hampshire (UNH), and others (Atmospheric Investigation, Regional Modeling, Analysis, and Prediction project (AIRMAP), The New England Air Quality Study, Draft Science Plan, October 2001, available at http://www.al.noaa.gov/neaqs/). For NEAQS, researchers at UNH's Climate Change Research Center created a mesoscale surface weather network by adding a series of small, automated stations to NOAA's existing network surface stations (Figure 4). The enhanced network of stations permits the resolution of meteorological features as small as 10 km across, particularly over land. Hourly reports from the combined network were interpolated onto a rectangular grid using standard techniques [*Barnes*, 1964], and the regridded data were examined for patterns of wind flow near Earth's surface.

[39] The 3 August 2002 event (Figure 5) most closely resembled the pure sea breeze. A high-pressure center was approaching southern New England from the west, setting up a shore-perpendicular ambient flow. At 1200 UTC (subtract 4 hours to convert to local daylight time (LDT)) the flow throughout most of the study area was northwesterly (Figure 5a). At 1600 UTC a region of light winds, *cyclonic* rotation, and low-level convergence developed in the southern half, ~10 km offshore (Figure 5b). By 1900 UTC, there was a well-developed sea breeze with a clearly defined inland convergence zone in the southern half and wind flow crossing the coast at a right angle (Figure 5c). The sea breeze was beginning to develop in the north as well. By 2300 UTC the wind direction within the SBC veered to a more southerly direction, causing the system to take on characteristics of the corkscrew sea breeze (Figure 5d). At latitudes where Coriolis is important, the sea breeze evolves to take on corkscrew characteristics under the influence of rotational forces.

[40] The 21 July 2002 event (Figure 6) most closely resembled the corkscrew sea breeze from its inception. A cold front was approaching New England from the west, and a high was to the south, setting up shore-parallel, southwesterly flow. At 1300 UTC the wind

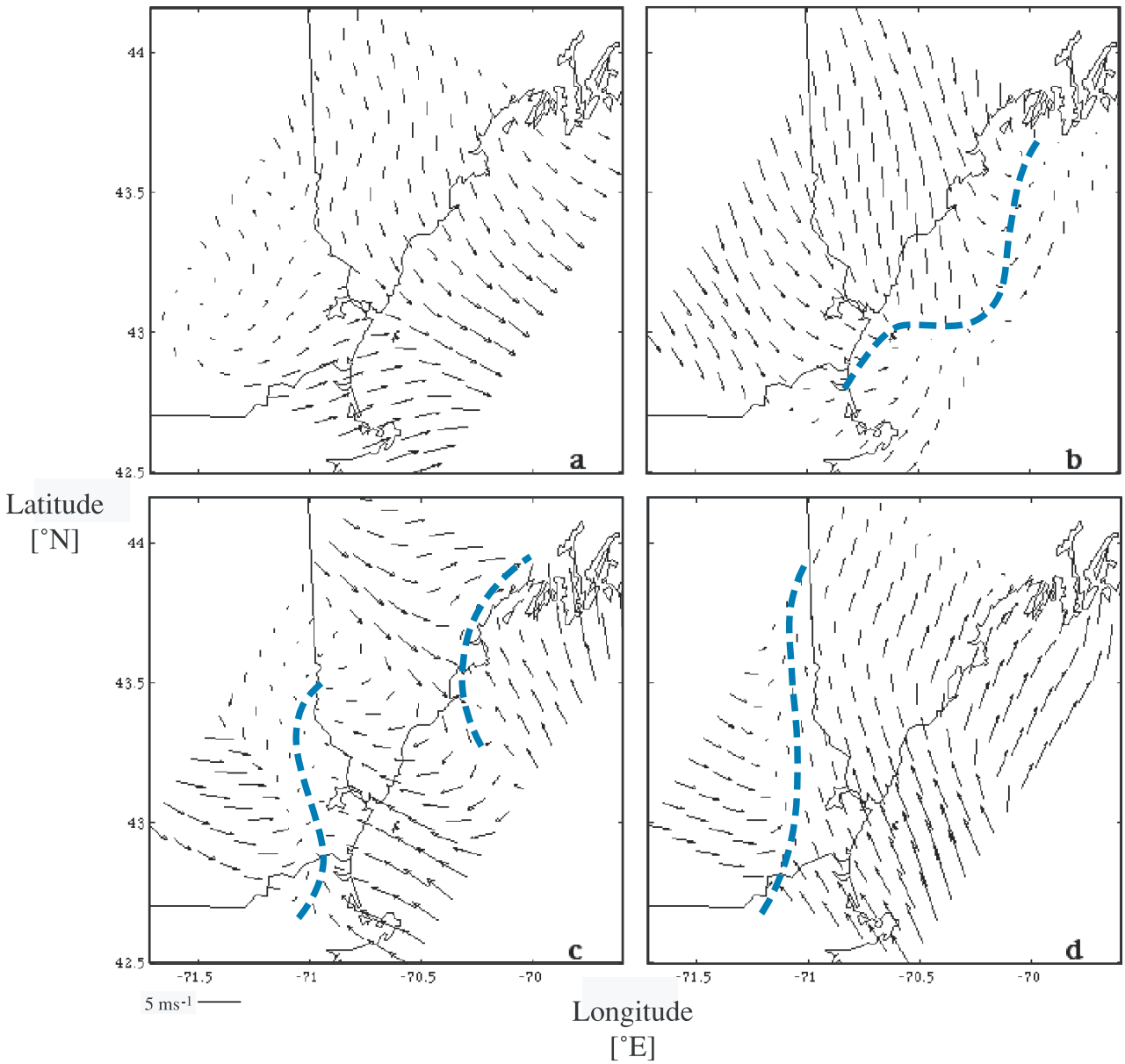

Figure 5. Pure sea breeze event 3 August 2002: (a) 1200 UTC (0800 LDT), (b) 1600 UTC, (c) 1900 UTC, and (d) 2300 UTC.

throughout the study area was southwesterly and shore-parallel (Figure 6a). By 1400 UTC the wind in the offshore area backed from southwest to southeast, developing a noticeable shoreward component and creating a pronounced convergence zone at the coast (Figure 6b). The SBC reached its peak at 2100 UTC, when the leading edge of the SBC extended inland nearly 65 km (Figure 6c) and thereafter began to diminish. By 0300 UTC on 22 July, *veering* wiped out the convergence zone, and the SBC was no longer readily identifiable (Figure 6d).

[41] The 24 July 2002 event (Figure 7) most closely resembled the backdoor sea breeze described in section 3.2.2.1. A high-pressure center was approaching northern New England from the west, setting up shore-parallel, northeasterly flow. At 1200 UTC the wind throughout most of the study area was northeasterly and shore-parallel (Figure 7a). By 1500 UTC, veering added a shoreward component throughout the southern half; therefore there was no well-defined line of convergence between the ambient flow over the continent and the flow within the developing SBC (Figure 7b). Continued veering rotated the wind from northeast to southeast by 2000 UTC, resulting in shore-perpendicular flow throughout the study area (Figure 7c). By 2300 UTC the demise of the SBC was marked by the collapse of organized flow on this scale (Figure 7d).

[42] These case studies indicate that the generic models introduced in the previous section are probably too simple for use other than in teaching basic concepts. In addition to along-shore variations, such as differing times of onset of the sea breeze, entire sea breeze events

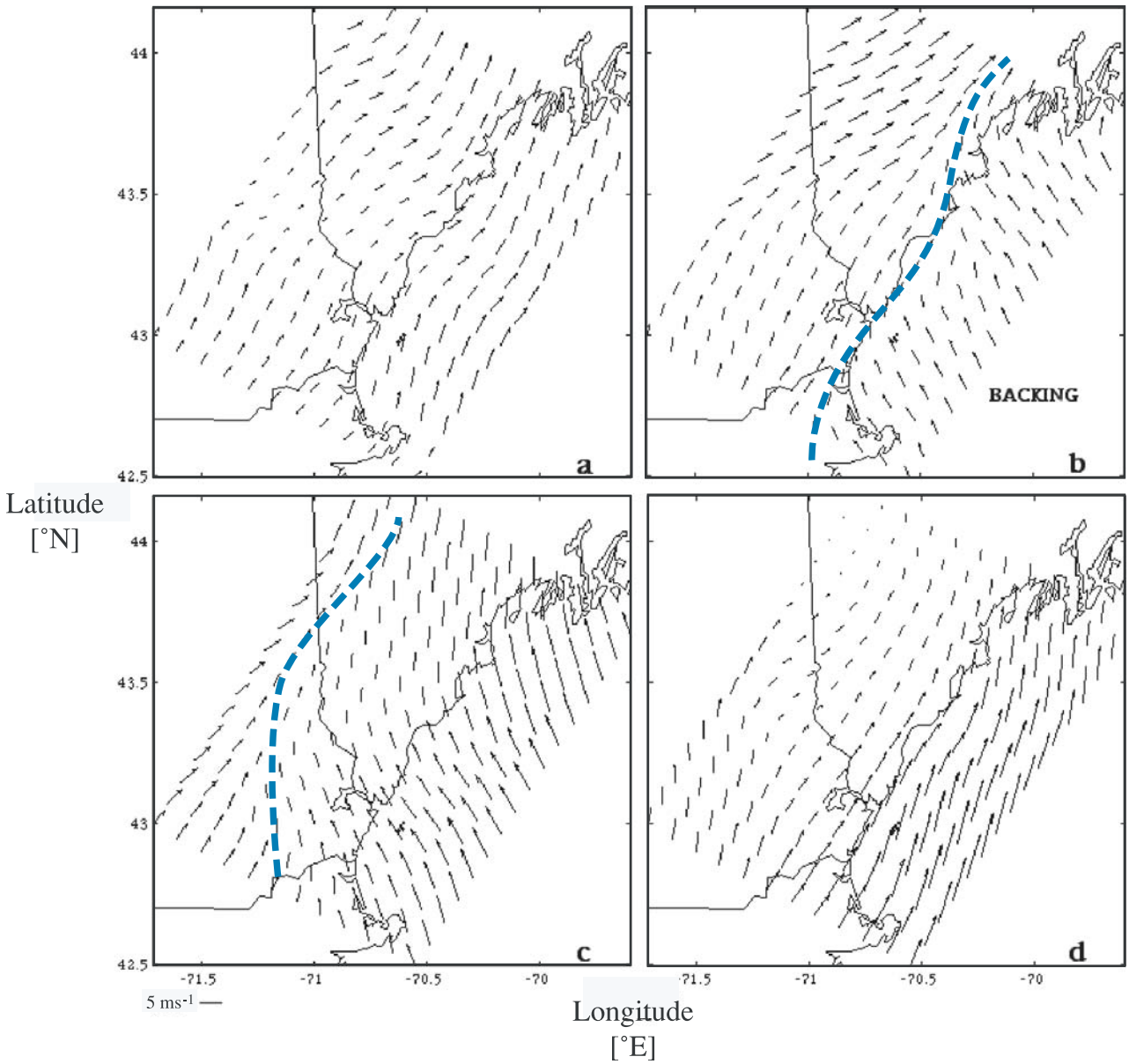

Figure 6. Corkscrew sea breeze event 21–22 July 2002: (a) 1300 UTC (0900 LDT), (b) 1400 UTC, (c) 2100 UTC, and (d) 0300 UTC.

evolve in ways not predicted by the generic models. The Coriolis force, which favors veering, is a dominant factor. In the 3 August (pure) sea breeze case, veering induced by the Coriolis force transformed the SBC from a pure into a corkscrew system. In the 21 July (corkscrew) case, backing occurred early in the life of the SBC, before Coriolis had time to become an important factor. (The Coriolis force requires several hours to become an important factor, a fact that can be derived by scaling the equations of motion.) The corkscrew sea breeze was terminated when the Coriolis force wiped out the cross-shore wind component. In the 24 July (backdoor) case, veering (driven by thermodynamic differences between land and sea) initiated the sea breeze, but the Coriolis force prevented backing from destroying it. Instead, the wind direction became random at the end of the SBC's life, driven by smaller-scale, local forces. The Coriolis force's influence on the SBS is discussed in greater detail in sections 3.4, 3.5.2.2, and 3.5.3.

3.2.3. Sea Breeze Gravity Current (SBG) and Kelvin-Helmholtz Billows

[43] The low-level landward flow of marine air is one example of a large class of phenomena called gravity or density currents. Gravity currents are primarily horizontal flows in fluids that can be generated by a density difference of only a few percent. Other examples of gravity currents are thunderstorm outflows, *turbidity currents*, avalanches, and *pyroclastic flows* [*Simpson*, 1997].

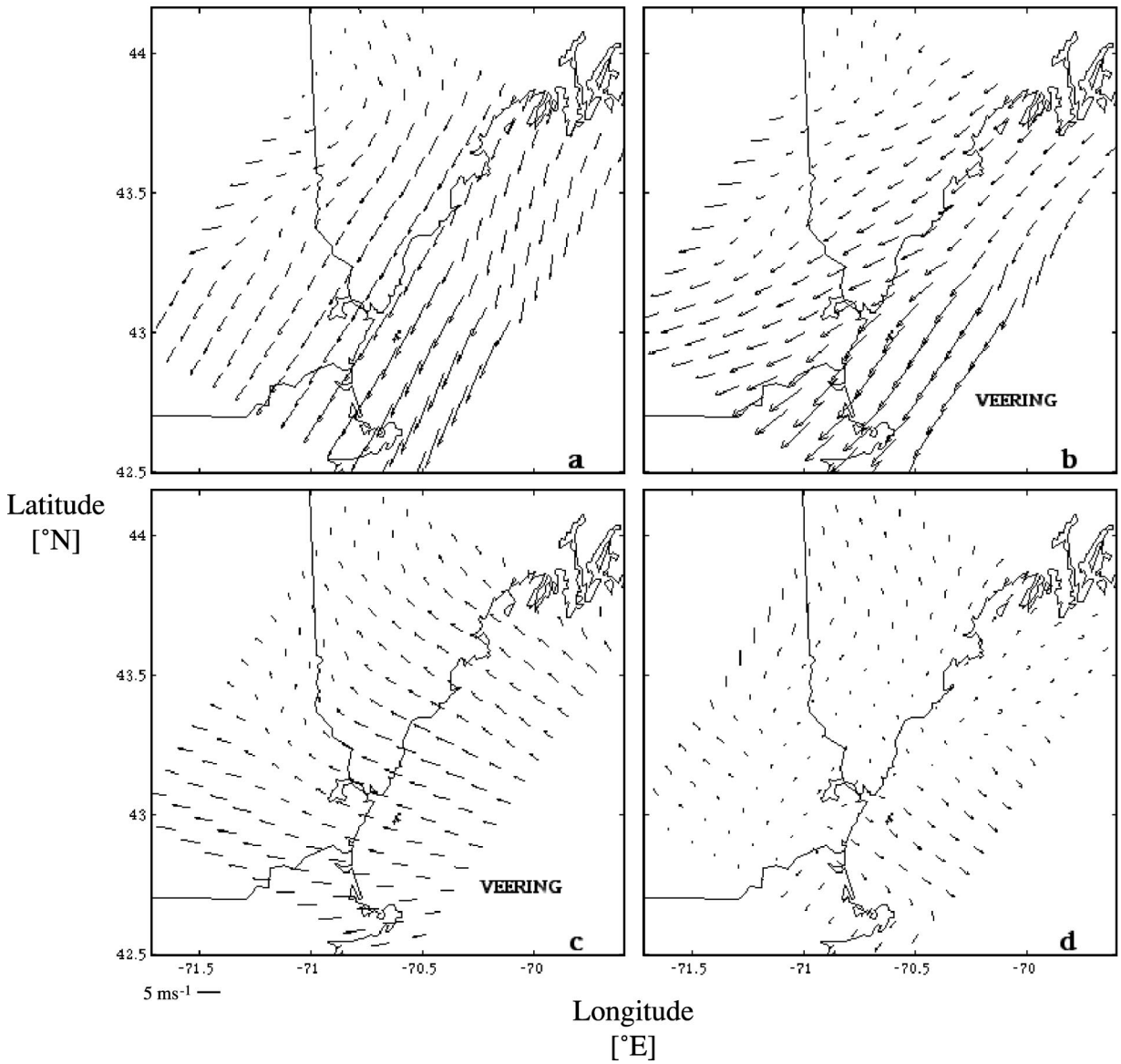

Figure 7. Backdoor sea breeze event 24–25 July 2002: (a) 1200 UTC (0800 LDT), (b) 1500 UTC, (c) 2000 UTC, and (d) 0000 UTC.

[44] The *microscale* (<2 km) horizontal thermal contrast across the boundary between marine and continental air masses can be very sharp, and the boundary often takes on a frontal nature similar to a *synoptic-scale cold front* [*Chiba*, 1993; *Finkele et al*., 1995; *Simpson*, 1997]. The leading edge of the marine air mass develops a raised head, because of the updraft created by low-level convergence between the marine and continental air masses [*Finkele et al*., 1995]. The height of the SBH is approximately twice that of the feeder flow originating offshore [*Simpson et al*., 1977], but a headwind (the ambient offshore flow) flattens the SBH [e.g., *Frizzola and Fisher*, 1963]. The depth of the onshore flow behind the front ranges between about 300 and 2500 m [e.g., *Barbato*, 1975]. *Simpson* [1969] noted that its average depth in Great Britain was ~700 m.

[45] The speed with which a density current advances into the ambient fluid has been studied extensively in the laboratory and the field [e.g., *Kuelegan*, 1957; *Simpson*, 1969; *Physick*, 1980; *Chiba*, 1993]. *Kuelegan*'s [1957] interest was the flow of salt water through locks and into freshwater channels, for which he established the following relationship:

$$|U| = k\sqrt{\frac{\Delta\rho}{\rho}\,gd}\,, \tag{5}$$

where $|U|$ is the speed at which the denser fluid front advances into the less dense fluid [m s^{-1}], k is a constant (taken as 0.78), ρ is the density of the denser fluid [kg m^{-3}], $\Delta\rho$ is the density difference between the two fluids [kg m^{-3}], g is the gravitational acceleration (9.81 m s^{-2}), and d is the height of the SBH [m].

[46] *Simpson* [1969] adapted equation (5) to describe the rate at which the SBG propagates inland. To calculate the constant k, he replaced the height of the SBH

(d) with its mean height $\bar{d}$, taken as 700 m (from a climatology of 54 sea breezes recorded over a 6-year period in Britain). He also replaced $\Delta\rho/\rho$ with $\Delta T/T$ [ΔT and T in kelvins]. This work yielded a k value of 0.62, which *Schoenberger* [1984] reported is equally effective when compared to radar observations of the propagation speed of a land breeze on the lower peninsula of Michigan.

[47] Later, *Simpson and Britter* [1980] determined that the SBG's rate of inland progression is slowed by ~3/5 of the opposing component of the PW or

$$|U| = k\sqrt{\frac{\Delta T}{T}\,g\bar{d}} - 0.59u_g, \tag{6}$$

where u_g is the cross-shore geostrophic wind component [m s^{-1}] resulting from the synoptic-scale PGF.

[48] A shear zone develops on the upper boundary of the marine air mass, between the low-level onshore flow and the seaward return flow aloft. KHBs develop in the shear zone over land (and are further enhanced by thermodynamic instability induced by insolation during the middle part of the day), causing mixing between marine air and continental air and creating a turbulent wake behind the SBH [*Simpson*, 1969; *Atkins et al.*, 1995; *Chiba et al.*, 1999]. The development of KHBs in late morning causes a friction-like force on the upper boundary of the air mass that slows the sea breeze's inland progression [e.g., *Sha et al.*, 1991]. KHBs appear as vortex rolls in regions of strong shear when the *Richardson number* (*Ri*), the ratio of static stability to kinetic energy of shear, is <0.25. This may be calculated by

$$Ri = \frac{\dfrac{g}{\bar{\theta}}\dfrac{\partial\theta}{\partial\theta}}{\left(\dfrac{\partial u}{\partial z}\right)^2}, \tag{7}$$

where g is the gravitational acceleration (9.81 m s^{-2}), θ is the *potential temperature* [K], u is the horizontal flow component [m s^{-1}], and z is the vertical dimension [m]. It can be seen from equation (7) that regions where the vertical temperature gradient vanishes, such as in a well-mixed layer resulting from convective overturning, are prone to the development of KHBs. *Simpson and Britter* [1980] suggested that the KHBs along the upper boundary of the sea breeze marine layer may be 500–1000 m in length. *Nielsen* [1992], using aircraft, observed KHBs with wavelengths between 1000 and 2000 m on the upper boundary of a New England coastal front, a mesoscale phenomenon that closely resembles a sea breeze.

[49] *Simpson* [1994, 1997] conducted experiments that documented the three-dimensional (3-D) structure of gravity currents, using laboratory tanks and two bodies of water of slightly different densities. His work reproduced several aspects of the SBG, including the SBH, front, and KHBs. Field studies have confirmed that analogs of Simpson's laboratory gravity current features (Figure 8) are also present in the SBG [e.g., *Craig et al.*, 1945; *Chiba et al.*, 1999; *Wood et al.*, 1999].

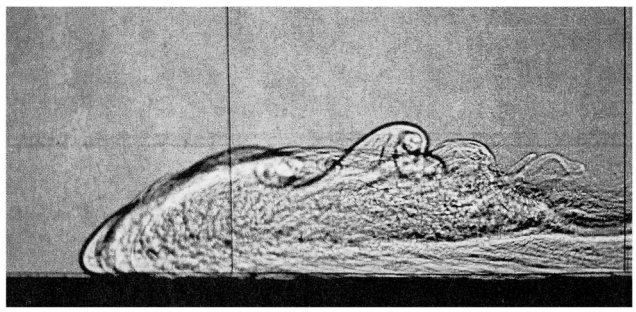

Figure 8. *Simpson*'s [1997] shadowgraph of a laboratory gravity current. Pure water is on the left, and slightly salty (denser) water enters from the right. Visible in the photograph are the current's nose (slightly elevated leading edge), raised head, and trailing Kelvin-Helmholtz billows (as described in text). Reprinted with the permission of Cambridge University Press.

3.2.4. Sea Breeze Front (SBF)

[50] The leading edge of the SBG is often associated with a strong cross-shore temperature contrast, and it can take on characteristics similar to those of a synoptic-scale cold front. As a front, the SBF is subject to *frontogenesis* and *frontolysis*, bifurcation (separation of the regions of maximum temperature gradient and maximum low-level convergence), variations in intensity (in terms of cross-shore width and the magnitude of the various gradients involved), and variations in slope. Strong vertical velocities and the SBH are associated with the SBF (Figure 9). The region of the SBG behind

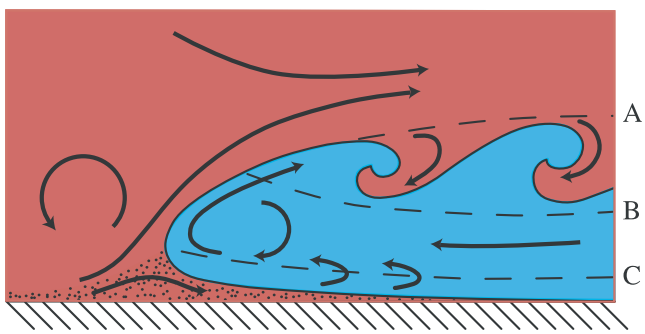

Figure 9. Simplified two-dimensional flow associated with a gravity current in presence of surface friction [after *Simpson*, 1997; *Sha et al.*, 1993]. Ambient fluid (red) is on the left and above. Denser fluid (blue) is invading from the right. Black arrows indicate direction of fluid flow. Mixing between the two fluids occurs both beneath the "nose" of the denser fluid (stippled, below line C) and in turbulent wake region behind the head of the gravity current (between lines A and B). Figure 9 was redrawn from *Simpson* [1997] with permission from the author.

the SBF and beneath the SBH can sometimes separate from the feeder flow and propagate inland as a *cutoff vortex* or undular bore. Sea breeze fronts vary in intensity in the along-shore direction, even along nearly homogeneous coasts.

3.2.4.1. Frontogenesis Function

[51] Sea breeze frontogenesis (the formation or intensification of the sea breeze front) can be defined as an increase in the magnitude of the cross-shore potential temperature gradient. A secondary set of processes involves the cross-shore water vapor gradient [e.g., *Kraus et al*., 1990]. A *kinematic* function describing the processes (not including the release of latent heat) that contribute to the thermal frontogenesis can be derived by beginning with the three-dimensional diffusion relation:

$$\frac{\partial Q}{\partial t} + u\,\frac{\partial Q}{\partial x} + v\,\frac{\partial Q}{\partial y} + w\,\frac{\partial Q}{\partial z} = K_x\,\frac{\partial^2 Q}{\partial x^2} + K_y\,\frac{\partial^2 Q}{\partial y^2} + K_z\,\frac{\partial^2 Q}{\partial z^2}, \qquad (8)$$

where Q is the heat content (energy) per unit volume [J m^{-3}], the first term on the left-hand side (LHS) is the time-dependent (Eulerian) term, and the remaining three terms on the LHS describe the horizontal and vertical advection of heat via wind components u, v, and w [m s^{-1}]. The three terms on the right-hand side (RHS) describe the turbulent diffusion of heat in three dimensions, with coefficients K_x, K_y, and K_z [m^2 s^{-1}] [*Anderson et al*., 1984]. All seven terms have overall units of power per unit volume [W m^{-3}].

[52] By assuming, (1) a north-south coastline with ocean on the right, (2) a weak north-south temperature gradient, (3) a wind primarily from the west ($v \sim 0$), and (4) $K_x \approx K_z$, relation (8) can be rewritten as

$$\frac{\partial Q}{\partial t} + u\,\frac{\partial Q}{\partial x} + w\,\frac{\partial Q}{\partial y} = K\left(\frac{\partial^2 Q}{\partial x^2} + \frac{\partial^2 Q}{\partial z^2}\right). \qquad (9)$$

[53] From here one may follow a line of reasoning similar to that of *Miller* [1948] and derive a function describing sea breeze frontogenesis. Since equation (9) describes heat, not heat gradient, the first logical step is to take the partial derivative in the cross-shore (x) direction. Assuming that K is approximately constant and following the chain rule for derivatives, equation (9) becomes

$$\frac{\partial Q_x}{\partial t} + \frac{\partial u}{\partial x}\,Q_x + u\,\frac{\partial Q_x}{\partial x} + \frac{\partial w}{\partial x}\,Q_z + w\,\frac{\partial Q_x}{\partial z} = K\nabla^2 Q_x, \qquad (10)$$

where ∇^2 is the second-order derivative in the x-z plane and subscripts (e.g., Q_x) indicate the partial derivative of the function (Q) in the direction indicated (x, z).

[54] By noting that the first, third, and fifth terms on the LHS of equation (10) constitute the material derivative of the quantity Q_x in the x-z plain and moving the remaining LHS terms to the RHS, the relation can be written as

$$\frac{\partial Q_x}{\partial t} = -\frac{\partial u}{\partial x}\,Q_x - \frac{\partial w}{\partial x}\,Q_z + K\nabla^2 Q_x. \qquad (11)$$

[55] *Reible et al*. [1993] began with equation (11) and then introduced scaling arguments to approximate the values of the terms on the RHS. *Kraus et al*. [1990] carried the argument further by using $Q_x = -c_p\rho_a\theta_x$ and $Q_z = -c_p\rho_a\theta_z$, where c_p is the coefficient of specific heat at constant pressure [J kg^{-1} K^{-1}], ρ_a is the density of air [kg m^{-3}], and θ_x and θ_z are the derivatives of the potential temperature field [K m^{-1}] in the x and z directions [*Halliday et al*., 1993]. These substitutions and algebraic manipulation lead to

$$\frac{d\theta_x}{dt} = -\frac{\partial u}{\partial x}\,\theta_x - \frac{\partial w}{\partial x}\,\theta_z + K\nabla^2\theta_x, \qquad (12)$$

which is the kinematic frontogenesis function. Term 1 on the RHS describes cross-shore confluence (or deformation); term 2 describes rotation of vertical temperature gradients into the horizontal plane; and term 3 describes cross-shore variations in turbulent heat diffusion [*Kraus et al*., 1990].

[56] With the ocean to the right (toward positive x values), sea breeze frontogenesis is indicated if the sum of the RHS is less than zero, and frontolysis (the destruction or weakening of the sea breeze front) is indicated if the sum of the RHS is greater than zero. In the former case the cross-shore potential temperature gradient is tending toward more negative values with time, and in the latter it is tending toward more positive values with time.

[57] There are two ways to improve this result. First, *Neumann* [1977] noted that within a few hours, even a system that begins with exclusively cross-shore flow will develop important flows and gradients in the along-shore direction, because of the rotation of the SBS under Coriolis and other forces. An improved kinematic frontogenesis function will account for horizontal rotation. Second, the assumption that the coefficient of turbulent diffusion is the same in both the horizontal and vertical dimensions may not be correct [e.g., *Anderson et al*., 1984]. An improved kinematic frontogenesis function will permit anisotropic coefficients. Both of these points indicate a need for a 3-D thermal frontogenesis function, even if the front initially forms parallel to the coastline.

[58] If one begins with equation (8) and follows a derivation similar to that shown above, keeping all three spatial dimensions and allowing $K_H \neq K_V$ (horizontal and vertical coefficients, respectively), one arrives at the following:

$$\frac{d\theta_x}{dt} = -\frac{\partial u}{\partial x}\,\theta_x - \frac{\partial v}{\partial x}\,\theta_y - \frac{\partial w}{\partial x}\,\theta_z + \frac{\partial}{\partial x}\left[K_H\,\frac{\partial^2\theta}{\partial x^2}\right]$$

$$+\frac{\partial}{\partial x}\left[K_H\frac{\partial^2\theta}{\partial y^2}\right]+\frac{\partial}{\partial x}\left[K_V\frac{\partial^{2\theta}}{\partial z^2}\right], \quad (13)$$

which is similar to equation (12). In equation (13) the RHS terms correspond to the following:

1. Term 1 is a cross-shore confluence (or deformation, as in equation (12)).

2. Term 2 is the rotation of along-shore temperature gradients into the cross-shore direction resulting from a cross-shore variation in the along-shore wind component. Along-shore gradients can result from rotation of the entire SBC, interactions between the advancing SBF and convective cells in the continental air mass, and the lobe and cleft structures observed on the front itself [*Neumann*, 1977; *Simpson*, 1997; *Stephan et al*., 1999].

3. Term 3 is the rotation of vertical temperature gradients into the horizontal plane (as in equation (12)).

4. Terms 4 and 5 are the cross-shore variation in cross- and along-shore eddy-driven heat diffusion.

5. Term 6 is the cross-shore variation in eddy-driven diffusion of heat in the vertical dimension.

[59] *Kraus* [1992], using data recorded by instrumented aircraft, computed the contribution to overall frontogenesis resulting from terms 4, 5, and 6 and determined that their contributions are of the same order of importance as the convergence and shear terms, at least in very sharp fronts. These terms can be either frontolytic or frontogenetic.

3.2.4.2. Frontal Bifurcation

[60] The sea breeze frontogenesis function (13) is a diagnostic tool, but there are a number of problems with attempting to use it for practical meteorology. Among them are the absence of a term for variations in along-shore gradients (which come into play in term 2), the absence of a term for shear due to along-shore variation in the cross-shore wind component (which will result in the rotation of horizontal temperature gradients), and the implicit assumption that the strongest temperature gradients and convergence zones associated with sea breeze fronts occur in the same place. The latter assumption is often not correct.

[61] More than one SBF may develop in a single SBS [e.g., *Kraus et al*., 1990; *Atkins et al*., 1995; *Lapworth*, 2000]. A field study of the SBF in eastern Florida, using Doppler radar stations and an instrumented aircraft, discerned a difference between the thermodynamic and kinematic fronts [*Atkins et al*., 1995]. The *thermodynamic front* is the location within the *planetary boundary layer* (PBL) where the mean thermodynamic properties of the air begin to differ from those of the ambient (continental) air, and it is created by interactions between the SBC and *horizontal convective rolls* (HCRs). The kinematic front is the location of maximum near-surface (100 m AGL) wind convergence. In an ideal case the two features are in the same place, and equation (13) diagnoses strong frontogenesis. In cases of onshore ambient flow the thermodynamic front may be as much as 15 km ahead of the kinematic front. The region between the two fronts (called the thermodynamic zone) is the analog of frontal transition zones in synoptic-scale cold fronts, and it is widest where the SBF has merged with HCRs [*Atkins et al*., 1995].

[62] *Atkins et al*. [1995] noted that only those cases with an offshore ambient wind exhibited the kinematic front. The lack of a clearly defined kinematic front may also be responsible for the apparent absence of a front in some of the sea breeze events noted elsewhere [e.g., *Helmis et al*., 1995].

3.2.4.3. Strength of the SBF

[63] Strong sea breeze fronts are those with (1) a significant temperature contrast between the two air masses, (2) a sharp temperature gradient (occurring over a narrow horizontal distance), or (3) both. The strongest fronts, most clearly identified by the frontogenesis function, will also be those where the thermodynamic and kinematic fronts are in the same place. At its simplest level these are the narrowest fronts. For narrow fronts to occur, strong low-level convergence is needed. Strong low-level convergence can occur with (1) strong, opposing offshore winds, (2) strong onshore winds within the marine air mass, or (3) both.

[64] *Helmis et al*. [1987] conducted a field study of the SBF in Athens, Greece, utilizing surface observations, an acoustic minisounder, and an atmospheric *turbulence* probe. They classify fronts into two groups, narrow and wide, that are dependent on the synoptic-scale wind direction. Narrower fronts with stronger temperature gradients occur when the synoptic-scale wind is offshore, and wider fronts with weaker temperature gradients occur when the synoptic-scale wind is parallel to the coast.

[65] *Chiba* [1993] studied the SBF in Japan through a full annual cycle and reports the width of the front as a function of the ratio U_C/U_M. U_C is the offshore wind speed in the continental air mass (observed before frontal passage), and U_M is the onshore wind speed within the marine air mass (observed after frontal passage). The wind speeds are recorded on a 21-m tower, 2 km inland from the coast. During the cold season (October through March) the ratio has typical values between 0.2 and 0.8, and during the warm season (April through September) it has values between 0.7 and 1.3. As the ratio increases from 0.7 to 2, the width of the SBF increases from 130 to 1120 m, with an overall average of 560 ± 230 m. This indicates that in the study area of *Chiba* [1993] the width of the front is inversely proportional to the relative strength (magnitude) of the onshore wind within the marine air mass and directly proportional to the offshore wind within the continental air mass.

3.2.4.4. SBF Slope

[66] The advancing SBF slopes backwards over the marine air at an angle of between 10° and 60° from the

horizontal [*Wood et al*., 1999; *Lapworth*, 2000]. Theoretical studies indicate the slope should be 60° near Earth's surface, with smaller values aloft [*Xu*, 1992]. These findings are mirrored in the laboratory tank experiments carried out by *Simpson* [1994, 1997]. Friction on Earth's surface reduces the forward momentum of the advancing front in the lowest few hundred meters (forcing the frontal surface toward the vertical), but aloft, in the absence of surface friction, the front moves inland more quickly, resulting in a leading nose with a much shallower slope above (Figure 8).

[67] *Wood et al*. [1999], from measurements made of the SBF in instrumented aircraft, reported a slope of 30° from the horizontal between 200 and 500 m AGL in one case but only 15°–20° in another. They speculated that the latter front had a shallower slope because it was moving across flat terrain, while the former was moving up a shallow incline, which reduced the front's forward momentum. An ambient opposing wind has a similar effect on the SBF. *Helmis et al*. [1987] observed that when the sea breeze advances into stronger opposing synoptic-scale winds, it exhibits a shallower slope (smaller angles from the horizontal), and a sea breeze moving into ambient shore-parallel wind regimes exhibits a steeper slope (larger angles from the horizontal).

3.2.4.5. Vertical Velocities at the SBF

[68] A scale analysis of the frontogenesis function reveals that the vertical shear term (involving cross-shore variations in the vertical component of velocity) is of the same approximate magnitude as the horizontal terms. Vertical currents initiated or enhanced by the SBF can cause convective clouds, including thunderstorms. (For more about the initiation of thunderstorms and other convective activity by the sea breeze front, see *Pielke* [1985], *Pielke et al*. [1991], *Rubes et al*. [1993], *Atkins et al*. [1995], *Weckwerth et al*. [1996], *Silva Dias and Machado* [1997], *Weckwerth et al*. [1997], *Carbone et al*. [2000], and *Rao and Fuelberg* [2000].) Vertical currents are also a factor in the dilution of pollutants in the PBL and are therefore of interest to air pollution meteorologists and engineers. Aviators are concerned about low-level wind shear resulting from sudden changes in vertical velocity. Therefore there are ample theoretical and practical reasons for studying the changes in the atmosphere's vertical motions brought about by the SBF.

[69] Figure 9 illustrates a simplified two-dimensional flow structure in a gravity current with bottom friction, representing a situation analogous to the sea breeze [*Sha et al*., 1993; *Simpson*, 1997]. Arrows indicate the direction of the fluid flow. The primary updraft is in the warm air immediately adjacent to the SBF. This updraft is caused by the physical wedge of the denser marine air undercutting the lighter continental air. Another updraft is in the cold air, immediately behind the SBF. This updraft is caused by low-level convergence and mass conservation, with thermal instability adding additional lift, and is the updraft responsible for the SBH. Additional, smaller-scale updrafts are visible behind the SBF, beneath the landward moving marine air mass, caused by surface friction and thermal instability. A prefrontal downdraft is visible inland of the primary updraft and is associated with prefrontal gravity waves [*Sha et al*., 1993]. This landward downdraft is part of a repeating pattern of updrafts and downdrafts in the continental air mass, associated with convective activity on a horizontal scale of ~2 km [*Stephan et al*., 1999]. Another downdraft is visible immediately seaward of the cold updraft within the sea breeze head, and together these form a closed vertical circulation [*Kitada*, 1987]. Pollutants can become trapped within this postfrontal *roll vortex* and be transported for great distances inland [*Kitada*, 1987]. Numerous updrafts and downdrafts are also visible in the turbulent mixing region associated with the KHBs.

[70] Before sea breeze frontal passage (fropa), downdrafts occur 60% of the time, while updrafts dominate after fropa [*Chiba*, 1993]. Observed downdrafts have had average magnitudes of ~0.5 m s^{-1}, while updrafts were between 0.5 and 1.0 m s^{-1} [*Chiba*, 1993; *Stephan et al*., 1999]. The magnitude of the vertical velocities is also dependent on the strength of the frontal zone and the rate at which the SBF advances inland [*Helmis et al*., 1987]. Vertical velocities of 1.0 to 1.5 m s^{-1} have been observed with sharp frontal zones, while weaker fronts produced updrafts and downdrafts only one third as large [*Helmis et al*., 1987]. Fast moving fronts produce greater vertical velocities than slow moving fronts [*Helmis et al*., 1987]. The direction of the ambient flow is also important, with updrafts as large as 2.0 m s^{-1} occurring at the SBF when the ambient flow is offshore [*Helmis et al*., 1987]. When the SBF interacts with HCRs, the largest upward vertical currents at the front occur where the frontal surface intersects an HCR rotating in the same sense as the postfrontal roll vortex [*Atkins et al*., 1995]. Regions of enhanced vertical velocities are marked by cumulus cloud development [*Atkins et al*., 1995].

3.2.4.6. Formation of Undular Bores

[71] During the late evening hours the SBF, SBH, and postfrontal roll vortex can separate from the feeder flow and continue moving inland independently as an *undular bore* or cutoff vortex [*Kitada*, 1987; *Simpson*, 1994]. The cutoff vortex is a solitary wave that propagates along the top of a low-level maritime or nocturnal radiation inversion [*Smith et al*., 1982] and is ~1 km high and ~20 km across in the cross-shore direction [*Sha et al*., 1993]. At ground level the approach of a cutoff vortex is marked by an abrupt increase in atmospheric pressure and temperature and a change in the wind speed and direction. Its arrival may or may not be followed later by the arrival of the sea breeze proper [*Simpson et al*., 1977; *Simpson*, 1996]. It often continues moving inland after the low-level onshore flow has ended, and it therefore is no longer part of a gravity current [*Abbs and Physick*, 1992].

Figure 10. Australian Morning Glory, as seen from the wing of a glider ~1 km above ground level. (Photograph courtesy of R. White.)

[72] *Simpson et al*. [1977] suggest that a cutoff vortex sometimes forms in southern England, shortly before sunset, but the most dramatic example of the phenomenon is the *Morning Glory* in the Gulf of Carpentaria region of northern Australia [e.g., *Smith et al*., 1982]. The Morning Glory occurs around sunrise, during the latter half of the austral dry season (mid-August through mid-November), and is associated with the sea breeze of the previous day. In addition to an abrupt pressure increase (sometimes exceeding 1 hPa in a few minutes) and shift in wind direction it is usually accompanied by one or more roll clouds roughly 1 km in height and many kilometers long (Figure 10), as well as intense wind squalls at the Earth's surface [*Smith et al*., 1982].

[73] Numerical model studies have determined two methods by which the sea breeze may contribute to the formation of undular bores. When two SBFs collide, or when one is overtaken by another, a hump of marine air is generated, eventually resulting in the conditions favorable for the formation of bores. In this case, two undular bores are created that move with approximately the same velocities as the original SBFs [*Clarke*, 1984]. Undular bores may also be created when the sea breeze penetrates inland and interacts with a nocturnal temperature inversion [*Sha et al*., 1993]. The interaction causes the SBH to detach and move inland, cut off from the low-level feeder flow. Eventually, the cutoff vortex dissipates from inertial damping and radiative energy loss [*Sha et al*., 1993]. Air pollutants emitted from ground sources within the marine layer can become trapped within the closed circulation behind the leading edge of the cutoff vortex [*Kitada*, 1987]. The vortex then serves as a mechanism that transports the pollutants inland. Downward vertical currents at the rear of the vortex move pollutants from the top of the PBL to the points closer to Earth's surface, even in thermally stable conditions [*Kitada*, 1987]. (The sea breeze's influence on air quality is discussed in greater detail in section 3.6.)

3.2.4.7. Along-Shore Variations in the SBF

[74] The cross-shore gradients of potential temperature, water vapor, and wind components associated with the SBF usually vary in magnitude in the along-shore direction. On a nearly homogeneous coast these variations are about 10 times smaller than the variations in the cross-shore direction. Along-shore variations in the SBF increase as the coastline becomes more complex. One cause of these variations is collisions between the SBF and convective elements in the continental air mass [*Stephan et al*., 1999]. The interaction between sea breeze fronts and convective activity is discussed in greater detail in section 3.3.

3.3. Interactions With External Meteorological Phenomena

[75] The SBS interacts with external meteorological phenomena at all stages of its life cycle. Within a short period of time following sunrise on days conducive to the formation of the SBS, cellular convection begins over land in response to surface insolation and low-level destabilization [*Mitsumoto et al*., 1983]. The cells have an aspect ratio of 1:1 and horizontal scales of 1–4 km and are sometimes visible as fair-weather cumulus [*Lyons*, 1972; *Mitsumoto et al*., 1983; *Stephan et al*., 1999]. A mixed layer of uniform thickness forms over land as a result of the convection, and the smaller cells merge into larger ones and attenuate [*Mitsumoto et al*., 1983]. The SBG moves into the well-mixed layer and interacts with the onshore convective disturbances, which, in turn, contribute to variations in the SBF's shape and speed [*Stephan et al*., 1999].

[76] The SBS may also interact with HCRs that develop in the convectively unstable continental air mass [*Atkins et al*., 1995]. During periods of ambient offshore flow the HCR rotation axes are nearly perpendicular to the SBF. As an HCR collides with the SBF, its axis of rotation is lifted upward from updrafts associated with the front. During periods of ambient onshore flow the HCR rotation axes are approximately parallel to the SBF. In this case, collisions between HCRs and the SBF constitute the merging of the two like-sign vortices and result in the strengthening of the SBF. Both scenarios result in the enhancement of cumulus clouds at the points of collision [*Atkins et al*., 1995].

[77] If the SBS develops near a coastal city, it will interact with the city's *urban heat island* (UHI). The presence of the UHI increases the sea breeze velocity during its growing stages [*Yoshikado*, 1992], and the acceleration increases as the size of the inland urban area increases [*Ohashi and Kida*, 2002]. The UHI also causes the SBC to last longer [*Ohashi and Kida*, 2002], and the interaction may result in unusually regular and persistent lines of clouds, such as the Kampachi Street cloud line in downtown Tokyo [*Kanda et al*., 2001].

[78] The SBS may interact with other thermally driven breezes, generated at points inland. *Zhong and Takle* [1992] conducted an observational study of SBS interac-

tions with river breezes in eastern Florida. The Indian River is a shore-parallel feature about 10 km inland, and it produces the largest of the river breezes in their study area. These authors found that the collision of the Indian River breeze (spreading outward perpendicular to the river's axis) with the Atlantic sea breeze creates areas of enhanced low-level convergence on both sides of the river. Smaller water features nearer the coastline produce minor atmospheric circulations that interact with the sea breeze, enhance low-level convergence, and speed up the inland movement of the SBF [*Zhong and Takle*, 1992].

[79] The low-level landward flow associated with the SBS interacts with the offshore temperature inversion separating the marine boundary layer from the air above it [*Barkan and Feliks*, 1993]. A field study in a harbor south of Tel Aviv, Israel, found that the marine inversion moved downward approximately *adiabatically* during the day, when the SBC was operating, and moved upward during the night, when the land breeze was in effect [*Barkan and Feliks*, 1993]. Model studies have shown that the portion of the marine inversion that varies diurnally extends >100 km offshore [*Feliks*, 1993].

[80] The SBS also interacts with synoptic-scale features. *Brümmer et al*. [1995] observed the interaction between the SBS and a synoptic-scale cold front (SSCF) that approached the northern coast of Germany from the North Sea. Before the relatively weak, shore-parallel SSCF arrived at the coast, the SBC was initiated between the marine air mass ahead of the SSCF and the continental air mass on shore. At about noon, as the SSCF approached the shore from the northwest, the SBF moved inland ahead of it. The onshore wind behind the SBF and ahead of the SSCF was so strong that the SSCF was subjected to a divergent wind field, resulting in the forward transfer of the thermal contrast associated with the SSCF to the SBF. At points inland later in the day, a single very strong frontal passage was observed [*Brümmer et al*., 1995].

3.4. Daily Life Cycle

[81] The life cycle of the SBS consists of five stages: immature, early mature, late mature, early degenerate, and late degenerate [*Clarke*, 1984; *Buckley and Kurzeja*, 1997]. These five stages apply to all three of the sea breeze categories described above. The land breeze, a near mirror of the sea breeze, evolves through a similar sequence of stages [*Holmer and Haeger-Eugensson*, 1999].

[82] During stage one, immature, the SBC begins as a divergence in the cross-shore wind component over the sea in response to the local-scale thermal PGF [*Clarke*, 1984]. The SBC expands more rapidly seaward than landward [*Finkele et al*., 1995]. Marine air moves onshore as a gravity current [*Simpson*, 1997], and the leading edge takes on frontal characteristics [e.g., *Kraus et al*., 1990; *Reible et al*., 1993]. Convergence in the cross-shore wind component develops over land, and the gravity current develops a raised head [*Finkele et al*., 1995].

[83] During stage two, early mature, insolation begins to decline, and the KHBs decay, removing the top friction and allowing the inland progression of the sea breeze to accelerate [*Clarke*, 1984; *Sha et al*., 1991; *Buckley and Kurzeja*, 1997]. During stage three, late mature, insolation drops toward zero, the land-sea thermal difference driving the SBC vanishes, the magnitude of the resulting landward force vector drops to zero, and supply of new marine air to the head of the sea breeze is cut off. However, the SBF remains sharp, and the center of the SBC cell shifts from a point near the coast to the landward edge of the marine air mass [*Clarke*, 1984]. After sunset, *radiational cooling* increases, which reduces vertical mixing and the associated updrafts and reduces the height of the SBH. The SBH continues to move inland [*Clarke*, 1984].

[84] During stage four, early degenerate, the SBH, now separated from the feeder flow and continuing to move inland independently, may interact with a nighttime radiational inversion or other low-level features and form a sea breeze cutoff vortex or undular bore [*Clarke*, 1984]. The most noted example of this phenomenon is the Morning Glory, which is discussed in section 3.2.4.6 [*Smith et al*., 1982; *Simpson*, 1994]. *Kitada* [1987] found that the undular bore can act as a pollutant transport mechanism, with descending currents at the rear of the cutoff vortex moving pollutants aloft down to Earth's surface.

[85] In the final stage, late degenerate, the circulation in the SBH is no longer closed [*Clarke*, 1984]. The leading edge flattens out, and Coriolis force rotates the flow and limits further penetration inland. At this stage the remnant of the sea breeze may also interact with developing nocturnal features, such as low-level jets and other gravity flows [*Clarke*, 1984; *Garratt and Physick*, 1985; *Buckley and Kurzeja*, 1997].

3.5. Forecasting

[86] The sea breeze is a standard forecast problem in coastal locations. Weather forecasters usually work under rather severe time constraints and therefore prefer simple, straightforward methods to complicated methods. There are several SBS forecasting techniques in the literature for specific locations that rely on meteorological variables included in standard surface and upper air observations. Unfortunately, local irregularities in the coastline and inland topography can have a strong effect on the SBS, so techniques developed for use in one location may not work well in another [e.g., *McPherson*, 1970; *Simpson*, 1994; *Miller and Keim*, 2003].

[87] Forecasting the sea breeze consists of at least three major components: (1) a simple yes/no (on whether or not it will occur), (2) the wind speed and direction, and (3) the distance of inland penetration during the day. The first question, whether or not a sea breeze will be observed at a given location, is also a

function of the last question. All three are discussed separately in sections 3.5.1, 3.5.2, and 3.5.3, respectively.

3.5.1. Occurrences

[88] A number of empirical studies examined the occurrence of the sea breeze as a function of land temperature, land-sea temperature difference, the strength of the opposing background (synoptically driven) wind, or some combination of these. The simplest approach uses the temperature information only. For example, *McKendry and Roulet* [1994] reported that all sea breezes observed on the western shore of James Bay were associated with inland temperatures >20°C.

[89] For it to be detected inland, the sea breeze must often blow upwind in opposition to the ambient flow. *Biggs and Graves* [1962] developed an early lake breeze forecasting index that compares the background wind to the land-sea temperature contrast:

$$\varepsilon = \frac{|U|^2}{C_p \Delta T}, \tag{14}$$

where ε is the lake breeze (*L-B*) *index* and represents the ratio of the inertial force ($\rho U^2/2$) and buoyancy force ($\rho g \beta \Delta T$, where β is the coefficient of expansion of air). $|U|$ is the near-surface wind speed [m s^{-1}], C_p is the specific heat coefficient of dry air at constant pressure (1.004 J g^{-1} K^{-1}), and ΔT is the difference between the inland air temperature and the temperature of the water surface ($T_{land} - T_{water}$) [°C]. Both $|U|$ and ΔT are determined by using a point far enough inland so that it is not affected by the sea breeze [*Simpson*, 1994]. If ε is large, then the inertial force is large, and there will not be a lake (sea) breeze. If ε is small, then the buoyant force is relatively large, and the lake (sea) breeze can move inland. Using a site on the west end of Lake Erie, *Biggs and Graves* [1962] found that the critical ε value is 3.0. If a transition zone between 2.7 and 3.2 is permitted, the L-B index correctly predicts the occurrence/nonoccurrence of the lake breeze 97% of the time [*Biggs and Graves*, 1962].

[90] *Lyons* [1972] recalibrated the L-B index for Chicago, Illinois (on the southwest shore of Lake Michigan), using a climatological record obtained during 10 summer months over a 2-year period (1966–1968). Rather than using an observed wind recorded at an inland surface site for the value of $|U|$, *Lyons* [1972] calculated the geostrophic wind speed using the 1200 UTC surface analysis. He reports a critical ε of 10.0, above which the lake breeze does not occur, which accurately forecasts the lake breeze 90–95% of the time. The difference between the critical value of *Lyons* [1972] and that reported by *Biggs and Graves* [1962] is attributed to the method used to determine $|U|$.

[91] Lake breezes and sea breezes are driven by the same mesoscale, thermally induced pressure gradients. *Simpson* [1994] repeated the L-B index calculations for the sea breeze at Thorney Island, Britain, and found a critical value of 7. Once again, the difference between Simpson's critical value and that reported by previous authors is attributed to the method used for obtaining $|U|$. In this case, rather than an observed surface wind or calculated geostrophic wind speed, *Simpson* [1994] used the 1000-m wind speed obtained with a pilot balloon ascent.

[92] About 60% of the forecast error by the L-B index is associated with the failure of the expected lake breeze to occur; that is, it overpredicts the lake breeze [*Biggs and Graves*, 1962; *Lyons*, 1972]. *Laird and Kristovich* [2001] examined this and related problems with the index using a 15-year climatology of the region surrounding Lake Michigan. They tested three variations on the L-B index, by computing it as originally described by *Biggs and Graves* [1962] (using $|U|$, the wind speed irrespective of wind direction), by substituting the observed cross-shore wind component U_x for U, and by substituting $|U_x|$, the magnitude of U_x, for $|U|$. The best results are obtained using U_x, and the worst results are obtained with $|U|$.

[93] *Laird and Kristovich* [2001] also reported three additional important findings. The first is that, although the lake breeze is driven by land-lake temperature differences (ΔT), large values of ΔT are not required, and in 70% of the lake breeze events in their climatology, daytime maximum ΔT values were <12°C. *Simpson* [1994] reports that temperature differences as small as 5°C are sufficient. A related result is that the lake breeze is always associated with relatively light ambient wind conditions; for example, for 95% of all lake breeze events the average daytime wind speed for the unaffected inland station was ≤5 m s^{-1}. Three quarters of all lake breeze events occurred when the cross-shore wind component had a magnitude ($|U_x|$) of 2 m s^{-1} or less. The third additional finding is that, in agreement with *Walsh* [1974], changes in location alone do not significantly affect the critical value of the index, meaning that for locations with similar topography and coastline shape the same critical L-B index value applies.

3.5.2. Surface Wind

[94] Once the forecaster has decided a sea breeze will occur, the next questions are of speed and direction. There are relatively straightforward methods for quantitatively estimating both of these in the literature. Speed and direction are considered separately in sections 3.5.2.1 and 3.5.2.2.

3.5.2.1. Speed

[95] One method of estimating the wind speed associated with the sea breeze is the Bjerknes circulation theorem, but it has already been shown that this greatly overestimates the surface wind (see section 3.1.2.). An alternative approach is to develop climatological records of the strength of the sea breeze and the temperature contrast between the inland air and the sea surface and then fitting a regression line relating the two data sets.

This is very straightforward, although it obviously must be repeated for each forecast site. *Mathews* [1982] developed a forecast rule for a Royal Australian Naval Air Station (RANAS) using this method. From a climatology of surface observations recorded over two summers at the Nowra RANAS, southeastern Australia, *Mathews* [1982] selected those days when the only important contribution to the 10-m wind was from the sea breeze. Wind speed was plotted as a function of the difference between the air temperature at the RANAS and temperature of the nearby ocean surface. A regression line resulted in

$$|U| = \frac{1}{2}\sqrt{\Delta T}, \tag{15}$$

where $|U|$ is the magnitude of the sea breeze component [knots] and ΔT is the land-sea temperature difference [°C].

[96] Another approach is to relate wind speed within the marine air mass to the speed of an advancing of SBG [e.g., *Simpson and Britter*, 1980]. *Keulegan*'s [1957] relation (5) describes the rate at which a gravity current advances into the ambient fluid. *Simpson* [1969] adapted this for forecasting the rate at which the SBG advances inland, and *Simpson and Britter* [1980] modified the relation to account for the opposing prevailing wind (equation (6)) and determined the relationship between the speed of the advancing sea breeze front and the wind velocity ahead of and behind it:

$$u_{\text{front}} \approx 0.87u_{SB} - 0.59u_g, \tag{16}$$

where u_{front} is the speed at which the sea breeze advances inland, u_{SB} is the wind speed within the marine air mass, and u_g is the cross-shore geostrophic wind component resulting from the synoptic-scale pressure pattern [*Reible et al*., 1993]. The two constants in equation (16) were determined by *Simpson and Britter* [1980] in laboratory studies using tanks of water.

[97] *Finkele* [1998], from a model study compared with in situ observations from aircraft, reported average speeds for the growth of the SBC of 1.6 m s^{-1} in the landward direction (slowing somewhat in the middle of the day) and compared this to a typical value of 3.4 m s^{-1} in the seaward direction. The former is comparable to u_{front}. *Simpson et al*. [1977], from field studies, reported that a typical value for u_{front} in England is about 3 m s^{-1}, and *Clarke* [1955] reported u_{front} values as high as 7 m s^{-1} in Australia. Several studies have reported variations in the speed of the front's inland propagation, slowing during the midday hours and regaining speed toward late afternoon, which is attributed to the development of Kelvin-Helmholtz billows along the top of the inland marine air mass and variations in soil moisture [*Physick*, 1980; *Sha et al*., 1991].

[98] Assuming that equation (6) represents the scalar speed at which the SBF moves inland, one can combine equations (6) and (16) to obtain

$$u_{SB} \approx \frac{k}{0.87}\sqrt{\frac{\Delta\rho}{\rho}\,gd}, \tag{17}$$

where k is a constant equal to 0.62 and d (the height of the SBH) can be replaced by a climatological mean ($\bar{d}$) without the loss of significant accuracy [*Simpson*, 1969].

3.5.2.2. Direction

[99] Two preliminary questions of interest are the following: (1) How does the surface wind direction change from the synoptically driven direction to the sea breeze direction? (2) What is the initial direction of the sea breeze once it is established? *McKendry and Roulet* [1994] addressed the first question in a field study conducted on the southwest shore of James Bay, where the coastline is fairly straight and oriented from south-southeast to north-northwest. They report that with a synoptic-scale wind that has a southerly component, the sea breeze is associated with backing (counterclockwise rotation) of the wind direction from the southern to the eastern quadrant. For a synoptic-scale wind with a northerly component the sea breeze is associated with veering (clockwise rotation) of the wind from the northern to the eastern quadrant.

[100] *McKendry and Roulet*'s [1994] results are logical when considered in the context of simple vector addition. Assuming that the Coriolis force is unimportant (at least initially) in the sea breeze, then the mesoscale flow will be parallel to the thermally induced pressure gradient toward lower pressure. In the case of a relatively uncomplicated coastline this implies a sea breeze wind vector directly perpendicular to the coast. For the net wind direction at any location, one must add the sea breeze wind vector to the synoptically produced wind vector to determine the net wind. In the case of a northerly synoptic-scale wind the growing sea breeze vector will gradually deform the net wind vector seen by a stationary observer in such a way that the net appears to rotate in a clockwise direction. With a southerly synoptic-scale wind the opposite is true.

[101] *Mathews* [1982] discussed vector addition in a practical technique for forecasting the direction of the sea breeze once it is established. The strength of the cross-shore sea breeze component is calculated by one of the methods discussed in section 3.5.2.1, and its direction is assumed to be directly perpendicular to the local coastline, with some small degree of variation. Then the sea breeze vector components are added to the gradient wind components, and the resultant wind is determined.

[102] Once the sea breeze is established, the associated wind direction may continue to rotate as the day progresses. Several field studies report a diurnal rotation in the sea breeze [e.g., *Pearce*, 1955; *Fisher*, 1960; *Zhong and Takle*, 1992; *McKendry and Roulet*, 1994]. Within the same hemisphere north or south of the equator the sense of the rotation may be either clockwise or the reverse and therefore cannot be accounted for by the Coriolis force alone. *Neumann* [1977] derived an expres-

Table 2. Varying Extent of the Sea Breeze's Inland Penetration in Different Parts of the World

Where	*Distance Inland, km*	*Reference*
Beaufort Sea coast, Alaska, United States	15	*Kozo* [1982]
Chicago, Illinois, United States (lake breeze)	40	*Lyons* [1972]
Indonesia	60–80	*Hadi et al.* [2002]
Southern England	100	*Simpson et al.* [1977]
James Bay, Ontario, Canada	100	*McKendry and Roulet* [1994]
Southeastern United States	150	*Buckley and Kurzeja* [1997]
Southeastern Spain	150	*Kottmeier et al.* [2000]
Australia	200	*Simpson* [1994]

sion describing the time evolution of the wind direction associated with the sea breeze for a north-south oriented coastline. The x and y axes correspond to the cross- and along-shore dimensions, respectively, and the expression takes the following form:

$$\frac{\partial \alpha}{\partial t} = -f + \frac{1}{|U|^2}\left[\frac{v}{\rho}\frac{\partial p_m}{\partial x} + f(uu_g + vv_g)\right], \quad (18)$$

where the LHS describes the rate and sign of the rotation [s^{-1}] and the three terms on the RHS are associated with (from left) (1) the Coriolis force, (2) thermally induced mesoscale PGF, and (3) synoptic-scale PGF. The angle between the wind vector and x axis is represented by α [radians], f is the Coriolis parameter ($= 2\Omega\sin\varphi$, where Ω is the rotational velocity of Earth and φ is latitude) [s^{-1}], $|U|$ is the scalar wind speed (net) [m s^{-1}], u and v are the cross- and along-shore components of the total wind vector [m s^{-1}], respectively, u_g and v_g are the cross- and along-shore components of the geostrophic wind vector [m s^{-1}], respectively, ρ is density [kg m^{-3}], and $\partial p_m/\partial x$ is the mesoscale pressure gradient resulting from the cross-shore temperature contrast [Pa m^{-1}]. Note that the third term on the RHS of equation (18) can also be written as

$$\frac{f(uu_g + vv_g)}{|U|^2} = \frac{1}{\rho|U|^2}\left(\frac{\partial p_L}{\partial x}v - \frac{\partial p_L}{\partial y}u\right), \quad (19)$$

where $\partial p_L/\partial x$ and $\partial p_L/y$ represent the synoptic-scale pressure gradients in the cross- and along-shore dimensions, respectively. A scale analysis reveals that the three terms on the RHS of equation (18) are within an order of magnitude of each other. Using data recorded in Nova Scotia, southern Australia, Washington state (United States), Scotland, and Great Britain, *Simpson* [1996] concluded that terms 1 and 2 are of comparable importance but that topographical influences can often be responsible for completely reversing the rotation imposed by all three terms.

[103] If the synoptic-scale pressure field is nonzero at the forecast location, then the best approach for determining the rotation imposed on the wind is to calculate the values of all three terms on the RHS of equation (18). For a few special cases, however, the solution is somewhat simpler.

[104] Consider the east coast of a continent in the Northern Hemisphere with no important variations in the shape of the coastline and no significant topography. If Coriolis clearly dominates, equation (18) becomes

$$\frac{\partial \alpha}{\partial t} = -f, \quad (20)$$

and the wind direction rotates clockwise (anticyclonically). Once rotation begins, then v (the along-shore component of the net wind vector) is nonzero. If the synoptic-scale pressure field is exceedingly weak, then the two components of the geostrophic wind are approximately zero, and equation (18) becomes

$$\frac{\partial \alpha}{\partial t} = -f + \frac{v}{\rho|U|^2}\left[\frac{\partial p_m}{\partial x}\right]. \quad (21)$$

With the ocean on the right, one can assume that in a sea breeze environment, $\partial p_m/\partial x$ is positive. Therefore, ignoring the Coriolis force for the moment, a positive (northward) along-shore component (v) implies counterclockwise (cyclonic) rotation, and a negative along-shore component implies clockwise (*anticyclonic*) rotation. Put another way, if the locally induced wind has a southward component, then the rotation imposed on the wind direction will be counterclockwise, but if the locally induced wind has a northward component, then the two terms in the RHS of equation (21) are at odds, and the net rotation imposed on the wind direction will depend on their relative magnitudes. Given that density (ρ) is nearly constant ($\sim$1.2 kg m^{-1} [*List*, 1968]) and f is constant for a fixed latitude, the terms that one must determine are v, $|U|$, and $\partial p_m/\partial x$.

3.5.3. Extent of Inland Penetration

[105] Forecasting whether the sea breeze will occur at an inland location is a problem of combining guidance from an index, such as equation (14), with an additional estimate of how far inland the sea breeze will penetrate during the day. Field studies have documented the extent of the sea breeze's inland penetration in different parts of the world (Table 2), but determining a set of generic governing principles is a very complex problem. By combining the results of several studies, *Simpson* [1994] found that the magnitude of the ambient cross-

shore wind component is an important control. With onshore synoptic-scale winds, inland penetration is limited to 30 or 40 km, possibly because the associated land-sea temperature contrast is weak. Conversely, an offshore wind of 7 m s^{-1} at 1000 m AGL limits inland movement to 20 km [*Simpson*, 1994].

[106] *Chiba et al*. [1999] conducted a field study utilizing an instrumented helicopter and expanded on *Simpson*'s [1994] general principles. From the results of several sea breeze case studies in Japan, *Chiba et al*. [1999] determined that the inland intrusion distance at midday is between 10 and 25 km, depending on the magnitude of the cross-shore synoptic-scale flow, atmospheric stratification, and geographical features in the area. Specifically, they noted the following: (1) With a strong offshore gradient and an unstable coastal layer the sea breeze's inland penetration is limited to 10 km; (2) when the atmosphere is stably stratified and the ambient flow is onshore at 6 m s^{-1}, the sea breeze reaches as far as 15 km inland; and (3) with high-pressure and light, offshore 850-hPa winds overhead the sea breeze reaches as far as 25 km inland.

[107] Field studies produce excellent results on the local behavior of the sea breeze, but computer models are better able to differentiate the many overlapping physical phenomena in the SBS and therefore are a better tool for determining the generic principles governing the sea breeze's inland extent. Some model studies focus on various phenomena that reach inland prior to the arrival of the sea breeze proper. *Tijm and van Delden*'s [1999] sound waves reach over 1000 km inland. *Geisler and Bretherton*'s [1969] sea breeze forerunner may reach as far inland as 60 km. Most modelers have focused on the SBC or the SBG.

[108] *Estoque* [1962], in a model study assuming a straight coastline and a hydrostatic atmosphere, concluded that an ambient offshore wind of 5 m s^{-1} limits SBC inland penetration to 18 km, while similar thermal forcing with calm ambient winds permits SBC inland penetration of 32 km. The former result closely parallels *Simpson*'s [1994] observation-based conclusions. In a comprehensive series of model studies, *Arritt* [1992] noted that an offshore ambient wind of ~1 m s^{-1} was conducive to the deepest inland penetration, peaking at >60 km. *Finkele* [1998] reported that the inland extent of the sea breeze is greater under light (2.5 m s^{-1}) ambient offshore wind conditions than in moderate (5 m s^{-1}) ones, but the seaward extent is similar in both situations. For strong offshore geostrophic winds (7.5 m s^{-1}) the SBC is entirely over the sea.

[109] *Pearce* [1955], using an early 3-D numerical model, determined that inland motion of the sea breeze is ultimately limited by Coriolis-induced rotation. *Rotunno* [1983] expanded on this, stating that where

$$f \geq \omega, \tag{22}$$

the sea breeze is confined to a finite distance from the coast determined by the vertical scale of heating and the static stability. Conversely, where

$$f < \omega \tag{23}$$

the sea breeze is in the form of internal waves that extend an "infinite" distance inland. In equations (22) and (23), f is the magnitude of the local Coriolis parameter ($= 2\Omega\sin\varphi$), and ω is the cycle of heating and cooling ($= 2\pi$ day^{-1}). Ω is the angular rotation of Earth, and φ is the latitude. It follows that the dividing line is where $4\pi\sin\varphi$ $day^{-1} \geq 2\pi$ day^{-1}, or $\sin\varphi \geq 1/2$, which is true if $\varphi \geq 30°$. For regions at and above 30° latitude, *Rotunno* [1983] concluded that the range of sea breeze's inland extent (L) near the ground is defined by

$$L = \frac{Nh}{\sqrt{\omega^2 - f^2}}, \tag{24}$$

where N is the Brunt-Väisälä frequency ($= \sqrt{(g/\theta)(\partial\theta/\partial z)}$) [$s^{-1}$] [*Rogers and Yau*, 1989] and h is the vertical scale of the heating [m]. *Dalu and Pielke* [1989] stated that friction limits both intensity (speed) and the inland extent. At the equator, where the Coriolis force is zero, the sea breeze is entirely limited by friction. Within 30° of the equator the "infinitely propagating" waves suggested by *Rotunno* [1983] may not appear because friction limits the sea breeze. By combining conclusions of the studies noted above with results of *McPherson* [1970], *Asai and Mitsumoto* [1978], *Mitsumoto et al*. [1983], *Sha et al*. [1991], *Zhong and Takle* [1992], *Arritt* [1992], and *Melas et al*. [1998], one can construct a summary of the controls on SBC inland propagation, shown in Table 3.

3.6. Air Quality Impact Mechanisms

[110] Meteorological and topographical features in coastal regions create complex low-level wind circulations. High concentrations of air pollutants are released into these circulations by industrial facilities (e.g., petrochemical plants, nuclear power stations, etc.), which are typically in or near urban areas and are often located near coastlines. Understanding the downwind behavior of these pollutants could assist in mitigating significant health problems [e.g., *Shearer and Kaleel*, 1982; *Clappier et al*., 2000]. The sea breeze has been implicated as either a direct control [e.g., *Kitada*, 1987; *Hsu*, 1988; *Physick and Abbs*, 1992] or as one contributing factor to more complex air quality scenarios [*Gaza*, 1998; *Seaman and Michelson*, 2000; *Gangoiti et al*., 2002].

[111] One example of a direct control is *Kitada*'s [1987] inland transport of pollutants by the postfrontal roll vortex. Another example is the convective internal boundary layer, also known as the thermal internal boundary layer. Cool, stable marine air encounters a thermodynamically unstable situation when it advects over a hot land surface. As the marine air mass moves inland and conducts heat from the land surface, convective currents begin to develop, and modified air is transported vertically. As the air moves farther inland, con-

Table 3. Summary of Controls on the Inland Penetration of the Sea Breeze

Control	*Description*
Magnitude and direction of the synoptic-scale cross-shore wind component	Seaward wind component of 7 m s^{-1} will limit inland penetration to 10 km or less. Light seaward wind component or calm ambient wind is most favorable for deep penetration. Seaward ambient wind component of 1 m s^{-1} may result in inland propagation of more than 60 km. Strong shoreward ambient wind is associated with weaker land-sea temperature contrasts and limits inland propagation to ~40 km.
Land-sea temperature contrast	There must be a positive land-sea temperature difference. Very strong temperature differences are not required. Minimum of 5°C is required for "deep" penetration.
Coriolis	Coriolis prevents SBC from extending inland "to infinity" by rotating associated wind until it is parallel to the coast.
Surface friction	Surface friction slows rate of inland movement and therefore extent SBC may reach before sunset, when thermal forcing is removed.
Top friction (KHBs)	KHBs slow rate of inland movement. KHBs form on SBH in low-stability conditions and propagate backward (toward sea) along top of SBG.
Thermodynamic stability in the continental air mass	Sea breeze may initially advance more readily into a well-mixed ambient air mass (often marked by fair-weather cumulus). Instability also gives rise to KHBs, which slow sea breeze's inland movement and therefore reduce the degree of penetration. Complex relationship between stability and penetration is discussed by *Rotunno* [1983], who predicts greater inland penetration in high-stability atmospheres but also in atmospheres with large vertical heating scale.
Shape of coastline	Inland bays along an otherwise straight coastline provide low-friction pathways for sea breeze to advance inland.
Topography	Terrain features can either assist or obstruct sea breeze's inland movement. If sea-facing hillside is relatively close to coast and is heated on the same diurnal cycle as adjacent coastal plain, resulting uphill wind current can assist the sea breeze's inland movement. If hill is in shadows, or shrouded in fog or clouds, it acts as an obstruction. Valleys funnel sea breeze, accelerating associated wind speeds, which carry marine air farther inland than would be the case over comparatively featureless terrain.
Interactions with other mesoscale systems	If sea breeze encounters other small-scale circulations, it is modified, and extent of its inland penetration may be either increased or reduced. For very weak sea or lake breeze, collision with thunderstorm downdraft may be enough to completely stop inland progression. Sea breeze's speed and direction of movement (and therefore its inland penetration) may be modified by collisions with other sea breeze systems, lake breezes, or river breezes generated at points inland.

vective currents reach progressively greater heights. The vertical overturning results in a CIBL near Earth's surface, whose upper limit increases nonlinearly with distance from the coast. Above the CIBL the remaining unmodified marine air acts as a cap that prevents mixing between destabilized marine air below and the continental air above [*Hsu*, 1988; *Stull*, 1988; *Prabha et al*., 2002].

[112] The CIBL is frequently the cause of persistent air pollution problems in coastal cities. The onset of the CIBL results in a dramatic reduction of the atmosphere's mixing depth, and locally generated pollutants trapped in the shallow surface layer can quickly reach unhealthy levels (Figure 11) [e.g., *Barbato*, 1975]. Pollutants such as sulfur dioxide (SO_2) and ozone (O_3) can be rapidly mixed to the surface when they encounter the convective currents within the CIBL [*Barbato*, 1975; *Gangoiti et al*., 2002]. *Fumigation* occurs when air pollution plumes emitted in stable regions of the marine air mass encounter the top of the CIBL and are rapidly mixed down to the surface (Figure 12) [*Lyons et al*., 1981; *Hsu*, 1988; *Abbs and Physick*, 1992; *Sawford et al*., 1998]. Plumes mixed to the surface may be vertically transported hundreds of meters aloft in updrafts associated with convection or lines of low-level convergence, then divided into multiple branches which move in many different directions. Some may eventually be caught up in the seaward return flow, transported many tens of kilometers offshore, and recirculated landward within the SBC cell. The pollutant concentration within the SBC can grow throughout the day as fresh emissions are fumigated downward into the CIBL, adding to older pollutants already in the SBS [*Shair et al*., 1982; *Panel on Coastal Meteorology*, 1992; *Abbs and Physick*, 1992].

[113] The variation in the height of the CIBL with distance from the coast is the subject of several field studies. *Raynor et al*. [1979] studied the CIBL over Long Island, New York, under a variety of prevailing wind and stability conditions. They found that the height of the CIBL (as a function of cross-shore distance) increases sharply near the coast but increases more gradually inland. *Druilhet et al*. [1982], using an instrumented aircraft, found that height of the CIBL increased as a

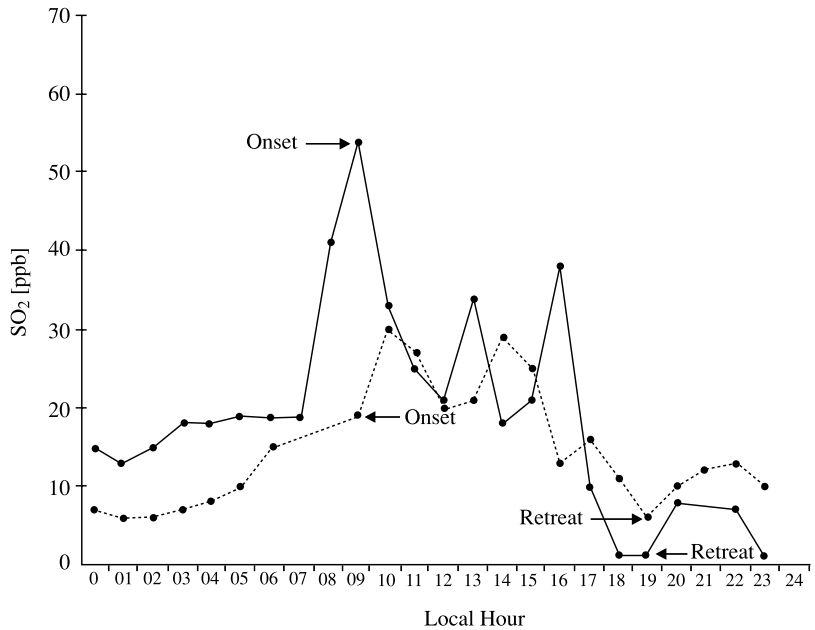

Figure 11. Atmospheric SO_2 concentration levels at two stations in Boston, Massachusetts. The concentration of SO_2 jumps dramatically following the passage of the sea breeze front (SBF) (indicated by "onset") because of fumigation induced by the convective internal boundary layer (CIBL). Plots are based on hourly SO_2 observations from September 1972 [after *Barbato*, 1975].

power of 0.4 of the cross-shore distance along the French Mediterranean coast. *Melas et al*. [2000] conducted a study of sea breeze behavior on the island of Sardinia and reported CIBL heights of ~50 m near the coastline, which increase gradually to over 500 m several kilometers inland. *Prabha et al*. [2002] reported CIBL heights between 150 and 200 m AGL, measured by a mini-SODAR positioned 5 km inland in the tropics. *Liu and Chan* [2002] studied internal boundary layers over Hong Kong and reported CIBL heights of up to 700 m AGL, reaching almost to the top of mountains in the complex terrain of the island.

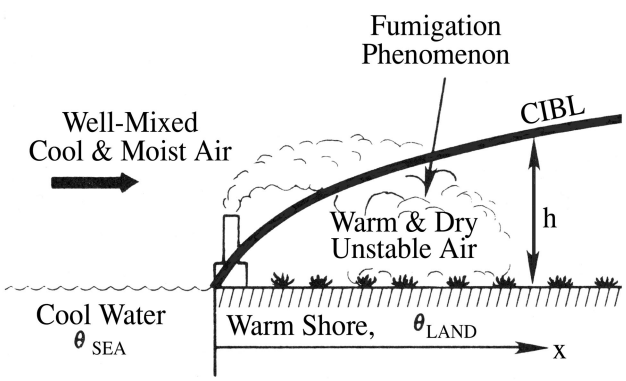

Figure 12. Convective internal boundary layer formed by advection of cool marine air over a warm land surface. Here "*h*" is the depth of the CIBL and varies as a function of distance from the coast (equations (25) and (26)). Details are given in text [from *Hsu*, 1988]. Reprinted with permission from Elsevier Science.

[114] In general, CIBL heights (h) grow as a function of the square root of distance from shore (x), but there are many modifying factors that scale the rate of growth. From first principles, *Venkatram* [1977] derived

$$h = \sqrt{\frac{2C_D(\theta_{\text{land}} - \theta_{\text{sea}})x}{\gamma(1 - 2F)}}, \tag{25}$$

where h and x are in meters, C_D is the drag coefficient ($\approx 12 \times 10^{-3}$), γ is the lapse rate above the boundary layer or over the water surface [K m^{-1}], F is the entrainment coefficient (0–0.22), and θ_{land} and θ_{sea} are the potential temperatures over the land and sea surfaces [K], respectively. *Hsu* [1988] evaluated the effectiveness of equation (25) by utilizing data from several field studies and reported that the observed CIBL heights and the theoretical predictions are in substantial agreement.

[115] *Melas and Kambezidis* [1992] evaluated equation (25) and several alternative models using data observed in Athens, Greece. They reported that the following relation, based on *Gryning and Batchvarova* [1990], is the most accurate predictor of CIBL height:

$$h = (1 - 0.002L_a)\sqrt{2C_DC_T(1 + 2A)} \times \sqrt{x\Delta\theta/\gamma} + 11\ln(-L_a), \tag{26}$$

where C_T is heat flux coefficient ($\approx C_D$) and A is a constant approximately equal to 2. L_a is given by

$$L_a = -\frac{(C_Du_h)^2}{k\dfrac{g}{T_0}C_T\Delta\theta}, \tag{27}$$

where u_h is the cross-shore wind component at the upper part of the CIBL [m s^{-1}], k is the von Kàrmàn constant (0.40), g is the gravitational acceleration (9.81 m s^{-2}), T_0 is the surface temperature [K], and $\Delta\theta$ is $\theta_{land} - \theta_{sea}$ [K] [*Melas and Kambezidis*, 1992]. *Luhar et al*. [1998] evaluated equation (26) using data recorded on the east coast of Australia. They found that it effectively predicted the observed CIBL height unless the atmosphere was neutrally stable, then a more complex model was needed.

[116] A number of additional studies have advanced the understanding of how the CIBL evolves. For example, *Raynor et al*. [1979], using an instrumented aircraft, found that the time rate of growth of the CIBL was initially slower with stable lapse rates over the sea than with neutral or unstable lapse rates. They also found that the height (h) of the CIBL does not grow to infinity with distance inland (as suggested by equations (25) and (26)) but reaches an equilibrium height that is dependent on downwind (inland) conditions. A higher CIBL is associated with low wind speeds and stronger land surface heating [*Raynor et al*., 1979]. *Federovich et al*. [2001], combining wind tunnel and numerical models, reported that the sign of the wind shear at the top of the CIBL affects the CIBL's rate of growth. Positive shear, where the wind momentum above the top of the CIBL is greater than within the CIBL, impedes the growth of the CIBL, when compared to the case when no wind shear is present. Negative shear, where the wind momentum within the CIBL is greater than above it, enhances the growth of the CIBL.

[117] A third example of a direct control by the sea breeze on air quality was studied by *Physick and Abbs* [1992]. They observed the behavior of pollutants released by power stations in the Latrobe Valley, southeastern Australia, over a 5-day period. The east-west Latrobe Valley extends more than 130 km inland and is bordered by mountains as high as 2000 m. An easterly sea breeze regularly penetrates >100 km up the valley, where it collides with an SBC moving inland from the south in the late afternoon. Observations indicated that the associated marine layer was ~1500 m deep. Westerly winds prevailed above 3000 m AGL during the study.

[118] The power stations are located ~90 km up the valley. The easterly SBG reaches this point by late afternoon, and the polluted valley air is lifted aloft and into the westerly return flow above the SBG. The marine air behind the SBF is cleaner than the valley air because (1) there are no additional pollution sources closer to the coast, (2) the top of the CIBL within the marine air is well below the top of the easterly SBG, preventing the downward convective mixing of pollutants, and (3) the combination of wind velocities aloft and offshore distances traveled makes recycling of the pollutants from the subsiding end of the SBC impossible [*Physick and Abbs*, 1992].

[119] The SBS can also become a factor in more complex air pollution scenarios. One of these occurs regularly on the east coast of the United States. *Pagnotti* [1987] describes the Appalachian lee trough (APLT), which forms along the eastern seaboard when the 700- to 500-hPa flow is southwesterly to northwesterly. The APLT causes the winds below 850 hPa to turn southwesterly, resulting in shore-parallel flow along the east coast, which, in turn, results in long-distance transport of O_3 and its precursors from the northeast urban corridor to rural areas farther up the coast [*Pagnotti*, 1987].

[120] The role played by the SBF in this scenario is documented in a case study of a July 1995 O_3 pollution event [*Gaza*, 1998]. *Gaza* [1998] used hourly observations of ground level O_3 concentrations at three locations on a line running north from New York City. O_3 concentrations spiked at each location as the SBF passed through (Figure 13). A horizontal contour analysis of O_3 concentrations revealed a front-parallel region of highly polluted air moving inland with the SBF. From additional case studies in the same region it became apparent that higher ground level O_3 levels occurred on days when the SBF was associated with well-defined low-level convergence. The highest O_3 levels occurred when the SBF moved inland and merged with the APLT [*Gaza*, 1998].

4. SUMMARY

[121] The sea breeze is a mesoscale wind that occurs at many coastal locations throughout the world. It develops when solar radiation and the differing rates at which land and water change temperature create a mesoscale pressure gradient force pointing toward the land. Cool marine air moves toward the land as a gravity current, is lifted vertically at the sea breeze front, and often forms a closed circuit via a return flow aloft and a diffuse region of descending currents several tens of kilometers out to sea.

[122] There are historical records documenting human understanding of the sea breeze system going back almost 2500 years, and it is still a rapidly evolving field. The SBS has been intensely studied since the beginning of the twentieth century, and more than 500 new papers have been published on the subject since 1990 alone, describing research using surface observations, balloon soundings of various kinds, aircraft, radar, lidar, and computer models. Modern researchers have been motivated by its influence on local wind velocity and air quality, convective activity, and other aspects of its dynamics and structure. Others have studied the sea breeze's influence on the coastal ocean and beaches. These authors have found that the SBS is a highly complex collection of nested phenomena, ranging in size from near synoptic to microscale. The SBS consists not only of the mesoscale *sea breeze circulation* (SBC), crudely described by the Bjerknes circulation theorem, but sound waves and other transitory wave-like phenomena that either initiate or are initiated by nonlinear responses of the atmosphere to diabatic heating. The SBC itself, sometimes called the sea breeze proper, is

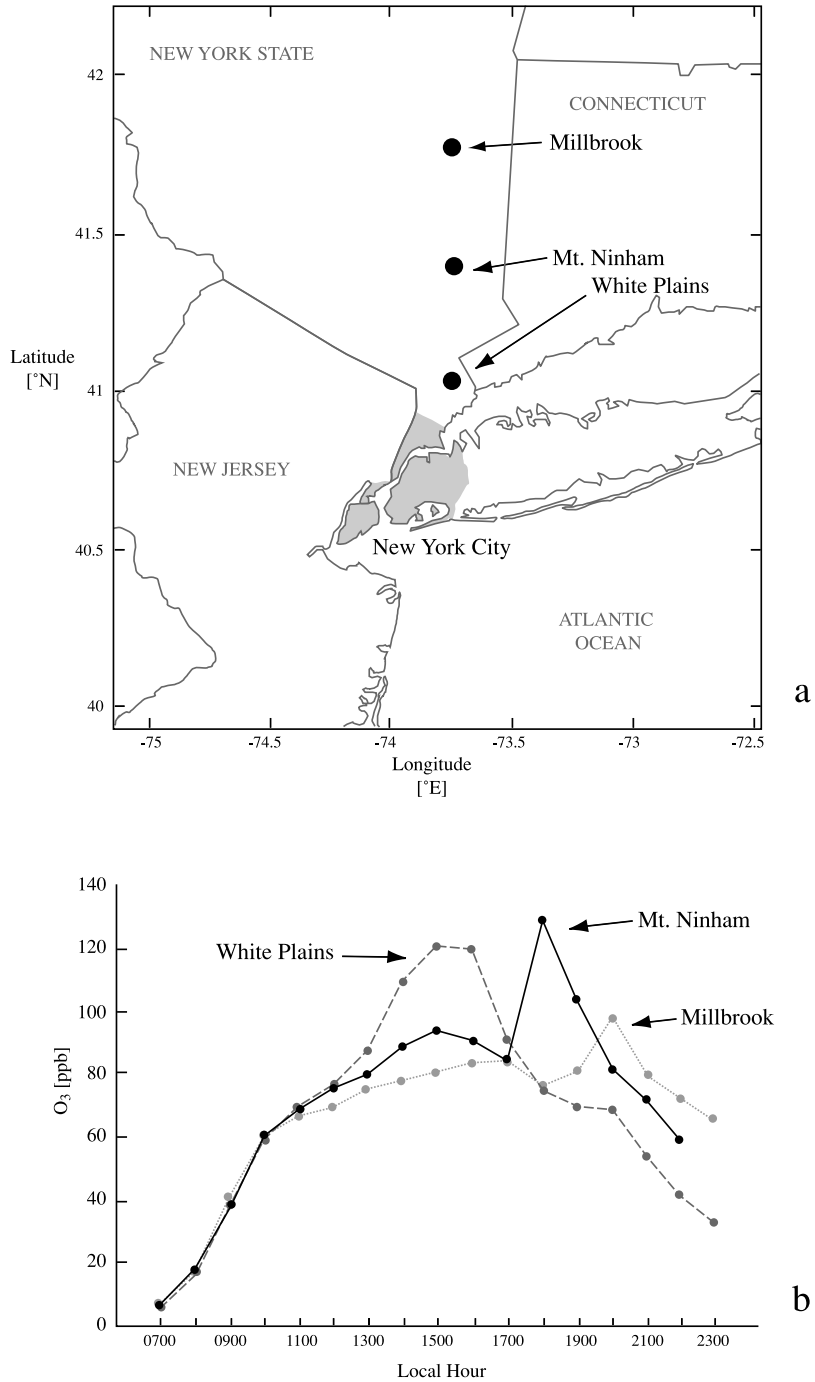

Figure 13. Ground level O_3 concentration levels at three stations north of New York City. (a) Locations of O_3 monitors in southern New York State. (b) Time series of O_3 concentrations. Note "spikes" as the SBF passes successively farther inland. Plots are based on hourly O_3 observations from July 1995. Figure 13 was redrawn after *Gaza* [1998].

distorted by nonzero ambient flow, forming helical circulations with both cross- and along-shore components. The SBC may not be a closed (mass conservative) circulation.

[123] The sea breeze gravity current (SBG) is the low-level landward flow of cool, moist marine air. The leading edge of the SBG is usually marked by a sea breeze frontal zone (SBF) that resembles a synoptic-scale cold front. The sea breeze front (SBF) may be bifurcated into a thermodynamic front and a kinematic front, where the former is the leading edge of the marine air's influence and the latter is the point of maximum low-level convergence between the marine and continental air masses. Strong vertical currents are associated with the front, creating a raised sea breeze head (SBH) above the SBF that may reach twice the height (up to 2200 m) of the feeder flow behind the SBF. The SBF and a vertically rotating postfrontal vortex within the marine air mass can sometimes separate from the feeder flow and move inland

independently as an undular bore. The most dramatic example of this is the Australian Morning Glory.

[124] Along the upper boundary of the SBG, Kelvin-Helmholtz billows (KHBs) develop when the Richardson number is smaller than ~0.25. Sea breeze–related KHBs have wavelengths between 500 and 1000 m and are responsible for mixing the two air masses in the turbulent wake zone behind the SBH. KHBs also generate a friction-like force along the top of the SBG that slows its inland progression during midday. A number of other instability phenomena can interact with the SBS, including vertical convection cells and horizontal convective rolls within the continental air mass.

[125] Forecasting the sea breeze is a three-part problem, consisting of determining (1) a simple yes/no for the shoreline, (2) the wind speed and direction behind the SBF, and (3) how far inland the sea breeze will penetrate. A simple index comparing the offshore wind component within the continental air mass to the magnitude of the cross-shore temperature gradient is very effective at answering the first question. The wind speed associated with the sea breeze can be calculated by a number of different methods, all of which are also dependent on the cross-shore temperature gradient, and the wind direction can be determined by an equation that accounts for rotation of the SBC under the Coriolis force, net along-shore wind component, and synoptic-scale PGF. In the absence of the latter two the entire SBC, and therefore the wind direction, will rotate anticyclonically over time. Determining the extent of the SBC's inland penetration is a complex problem, dependent on land-sea temperature contrast, the Coriolis force, surface and top friction, stability, and other factors. While theoretical relationships exist to determine the maximum possible inland penetration, accurate forecasts are still dependent on a field study for the site in question.

[126] The sea breeze exerts both direct and indirect controls on the fate of pollutants released into the coastal atmosphere. Examples of direct controls are the landward transport of pollutants by elements of the SBS, trapping and concentration of pollutants in shallow convective internal boundary layers, and replacement of polluted continental air with relatively clean marine air. The east coast of the United States is the site of a more complex air pollution problem, involving the sea breeze and a larger mesoscale trough that forms east of the Appalachian Mountains. A significant portion of the world's population resides in coastal areas, often side by side with industrial sites, ensuring that the sea breeze will be the subject of increasingly sophisticated research for some time to come.

Notation

C_a	circulation.
c_p	specific heat coefficient of air (constant pressure).
C_D	drag coefficient.
C_T	heat flux coefficient.
d	vertical depth of sea breeze.
$\overline{d}$	mean vertical depth of sea breeze.
D/Dt	material derivative.
f	Coriolis parameter.
F	entrainment coefficient.
g	gravitational acceleration.
h	height of CIBL.
H	horizontal scale.
k	constant, von Karman constant.
L	vertical scale.
P, P_0, P_1	atmospheric pressure.
Q	heat.
R	specific gas constant for air.
t	time.
T, T_1, T_2	temperature.
$\overline{T}1$, $\overline{T}2$	mean temperature.
u	eastward component of net wind vector.
$\overline{U}$	mean wind speed.
$\lvert U\rvert$	scalar wind speed.
u_{front}	rate of advance of sea breeze front.
u_g	eastward component of geostrophic wind, cross-shore wind speed in continental air mass.
U_h	cross-shore wind component at upper part of CIBL.
u_{SB}	wind velocity behind sea breeze front.
v	northward component of net wind vector.
v_g	northward component of geostrophic wind.
w	vertical component of net wind vector.
x	cross-shore dimension.
y	along-shore dimension.
z	vertical dimension.
α	angle.
β	expansion coefficient of air.
ε	lake breeze index.
φ	latitude.
γ	vertical temperature lapse rate.
K, K_H, K_V	coefficient of heat diffusion.
θ	potential temperature.
ρ, ρ_a	air density.
ω	diurnal cycle of heating and cooling

GLOSSARY

Adiabatic: A process in which a system (or parcel of air) does not exchange energy with its surroundings.

Anticyclonic: Horizontal circulation associated with areas of high atmospheric pressure and clockwise (counterclockwise) rotation in the Northern (Southern) Hemisphere.

Appalachian lee trough (APLT): A trough of low pressure that forms east of the Appalachian mountains

on days when the 700–500 hPa flow has a significant westerly component.

Backing: Counterclockwise rotation of the wind direction.

Buys-Ballot's law: A law describing the geostrophic wind. If you stand with your back to the wind in the Northern Hemisphere, lower pressure is on your left, and higher pressure is on your right. The relation is reversed in the Southern Hemisphere.

Circulation: A scalar quantity that represents a macroscopic measure of rotation over a finite area of fluid in two dimensions.

Coastal upwelling: See upwelling.

Convection: Vertical heat transfer by fluid flow. This occurs when the atmosphere is thermodynamically unstable, i.e., when warmer (lighter) air underlies colder (denser) air.

Convective internal boundary layer (CIBL): Well-mixed region within the marine air mass over land, adjacent to Earth's surface.

Coriolis force: An apparent force causing objects moving over the surface of Earth to be deflected to the right in the Northern Hemisphere and to the left in the Southern Hemisphere.

Cu: Fair-weather cumulus.

Cutoff vortex: See undular bore.

Cyclonic: Horizontal circulation associated with areas of low atmospheric pressure and counterclockwise (clockwise) rotation in the Northern (Southern) Hemisphere.

Diabatic: A process in which a system (or parcel of air) exchanges energy with its surroundings.

Diffusion: The transport of matter solely by random motions of individual molecules (also known as molecular diffusion) or due to the effects of turbulent motion (also known as dispersion).

Ekman pumping: Upward or downward vertical motion in the surface ocean resulting from the balance of the Coriolis force and wind stress on the sea surface.

Frontogenesis: The formation or amplification of a front due to an increase in the magnitude of the associated gradients. Results from the convergence of two dissimilar air masses.

Frontolysis: The dissipation or weakening of a front due to a decrease in the magnitude of the associated gradients.

Fumigation: Rapid downward mixing of an elevated plume of air pollution as it crosses from a stable layer into a turbulent mixed layer, such as a convective internal boundary layer.

Geostrophic wind: Theoretical wind resulting from balance between the horizontal pressure gradient and Coriolis forces.

Gravity current: A flow driven by horizontal density contrasts.

Hectopascal (hPa): Unit of pressure equivalent to 100 Pascals or one millibar. The mean atmospheric sea level pressure on Earth's surface is about 1013 hectopascals.

Horizontal convective roll (HCR): Overturning cylindrically shaped wind structures whose axis of rotation is parallel to Earth's surface.

Hydrostatic: Theoretical condition wherein the vertical pressure gradient force is balanced by gravity. There is no net vertical acceleration.

Inviscid: An inviscid (or ideal) fluid is one in which all surface forces exerted on the boundaries of each small element of the fluid act normal (perpendicular) to these boundaries.

Isobar: A line of equal atmospheric pressure.

Isotropic: Having the same properties in all directions.

Kelvin-Helmholtz billow (KHB): Wave structures seaward of the sea breeze head along the top of the sea breeze gravity current.

Kinematic: Pertaining to pure motion without regard to force, momentum, or energy.

Kinematic (sea breeze) front: The location of maximum near-surface (100 m AGL) wind convergence.

L-B index: Lake breeze index.

Mesoscale: Size scale of meteorological phenomena between 2 and 2000 km across. The meso-α scale consists of phenomena between 200 and 2000 km across, the meso-β scale consists of phenomena between 20 and 200 km across, and the meso-γ scale consists of phenomena between 2 and 20 km across.

Mesoscale pressure gradient force (mesoscale PGF): Pressure gradient force created by the local density difference between the marine and continental air masses. It points from the sea to the land.

Microscale: Size scale of meteorological phenomena less than 2 km across.

Morning Glory: Pronounced undular bore that occurs in northern Australia.

New England Air Quality Study (NEAQS): Joint project of the U.S. National Oceanic and Atmospheric Administration, the University of New Hampshire, and others to understand the interrelationships in New England's air quality, meteorology, and climate phenomena.

Nocturnal stable layer: Shallow, thermodynamically stable region of the atmosphere in contact with Earth's surface that is created by the emission of infrared radiation during hours of darkness.

Planetary boundary layer (PBL): Region of the troposphere directly influenced by Earth's surface.

Potential temperature (θ): The temperature a parcel of air would have if it were transported adiabatically to 1000 hPa.

Pressure gradient force (PGF): Horizontal force pointing from higher pressure to lower pressure, perpendicular to the isobars.

Prevailing wind (PW): Wind flow resulting from synoptic-scale systems.

Pyroclastic flow: Downslope flow of hot volcanic ash and cinders.

Radiational (or radiative) cooling: The nocturnal emission of infrared radiation from Earth's surface. It typically occurs on calm, clear nights and results in a nocturnal stable layer.

Richardson number (***Ri***): The ratio of static (thermodynamic) stability to kinetic energy of shear.

Roll Vortex: See Undular Bore.

Sea breeze circulation (SBC): Vertically rotating, closed circuit of wind flow caused by a mesoscale cross-shore temperature gradient.

Sea breeze front (SBF): The landward edge of the sea breeze system. The SBF consists of two main components: The thermodynamic SBF (SBFth) and the kinematic SBF (SBFkn). The former is characterized a strong cross-shore temperature gradient and marks the landward edge of the sea breeze gravity current. The latter is characterized by a change in wind direction and speed and marks the landward edge of the sea breeze circulation.

Sea breeze gravity current (SBG): Landward movement of cool marine air near Earth's surface.

Sea breeze head (SBH): The raised wave-like structure at the leading edge of the sea breeze gravity current.

Sea breeze system (SBS): Includes all aspects of the group of phenomena collectively called the sea breeze.

Synoptic-scale cold front (SSCF): The boundary between two synoptic-scale air masses, with the colder (denser) air mass advancing onto an area of Earth's surface previously dominated by the warmer (lighter) air mass.

Synoptic scale: Size scale of meteorological phenomena more than 2000 km across.

Thermal pressure gradient force (thermal PGF): See mesoscale pressure gradient force.

Thermodynamic (sea breeze) front: The location within the PBL where the mean thermodynamic properties of the air begin to differ from those of the ambient (continental) air.

Thermodynamic stability: The ability of a fluid to become turbulent or laminar because of the effects of buoyancy, a measure of the potential for convective overturning in a region of the atmosphere.

Turbidity current: Gravity current in which a limited volume of turbid (muddy) water moves relative to the surrounding water because of the current's greater density.

Turbulence: Irregular, unpredictable fluctuations in fluid media, generally occurring in all three spatial dimensions.

Undular bore: A solitary wave that forms when the leading edge of the SBG (beneath the SBH) separates from the remainder of the marine air mass and propagates inland independently.

Upwelling: The vertical transport of subsurface water to points nearer the sea surface.

Urban heat island (UHI): Region of atmosphere above and near urban areas that, because of the presence of urban structures, is warmer than the air above the surrounding countryside.

Veering: Clockwise rotation of the wind direction.

[127] **ACKNOWLEDGMENTS.** We would like to thank Frank Colby and James Koermer for their editorial assistance with this work. Figure 10 was reprinted from www.dropbear.com, with permission from Russell White. This review was produced for the Atmospheric Investigation, Regional Modeling, Analysis, and Prediction (AIRMAP) Project and was supported by NOAA grants NA07RP0475 and NA17RP1488.

[128] Kendal McGuffie was the Editor responsible for this paper. He thanks three technical reviewers and one cross-disciplinary reviewer.

REFERENCES

Abbs, D. J., and W. L. Physick, Sea-breeze observations and modelling: A review, *Aust. Meteorol. Mag.*, *41*, 7–19, 1992.

Adams, E., Four ways to win the sea breeze game, *Sailing World*, *March*, 44–49, 1997.

Anderson, D. A., J. C. Tannehill, and R. H. Pletcher, *Computational Fluid Mechanics and Heat Transfer*, 599 pp., Taylor and Francis, Philadelphia, Pa., 1984.

Angell, J. K., and D. H. Pack, A study of the sea breeze at Atlantic City, New Jersey using tetroons as Lagrangian tracers, *Mon. Weather Rev.*, *93*, 475–493, 1965.

Anthes, R. A., The height of the planetary boundary layer and the production of circulation in a sea breeze model, *J. Atmos. Sci.*, *35*, 1231–1239, 1978.

Apel, J. R., *Principles of Ocean Physics*, 634 pp., Academic, San Diego, Calif., 1987.

Arritt, R. W., Effects of the large-scale flow on characteristic features of the sea breeze, *J. Appl. Meteorol.*, *32*, 116–125, 1992.

Asai, T., and S. Mitsumoto, Effects of an inclined land surface on the land and sea breeze circulation: A numerical experiment, *J. Meteorol. Soc. Jpn.*, *56*(6), 559–570, 1978.

Asimakopoulos, D. N., C. G. Helmis, K. H. Papadopoulos, J. A. Kalogiros, P. Kassomenos, and M. Petrakis, Inland propagation of sea breeze under opposing offshore wind, *Meteorol. Atmos. Phys.*, *70*, 97–110, 1999.

Atkins, N. T., R. M. Wakimoto, and T. M. Weckwerth, Observations of the sea-breeze front during CaPE, part II: Dual-doppler and aircraft analysis, *Mon. Weather Rev.*, *123*, 944–969, 1995.

Banta, R. M., L. D. Olivier, and D. H. Levinson, Evolution of the Monterey Bay sea-breeze layer as observed by pulsed doppler radar, *J. Atmos. Sci.*, *50*, 3959–3982, 1993.

Barbato, J. P., The sea breeze of the Boston area and its effect on the urban atmosphere, Ph.D. dissertation, Boston Univ., Boston, Mass., 1975.

Barkan, J., and Y. Feliks, Observations of the diurnal oscillation of the inversion over the Israeli coast, *Boundary Layer Meteorol.*, *62*, 393–409, 1993.

Barnes, S. L., A technique for maximizing details in numerical weather map analysis, *J. Appl. Meteorol.*, *3*, 396–409, 1964.

Biggs, W. G., and M. E. Graves, A lake breeze index, *J. Appl. Meteorol.*, *1*, 474–480, 1962.

Brümmer, B., B. Hennemuth, A. Rhodin, and S. Thiemann, Interaction of a cold front with a sea-breeze front: Observations, *Tellus, Ser. A*, *47*, 383–402, 1995.

Buckley, R. L., and R. J. Kurzeja, An observational and nu-

merical study of the nocturnal sea breeze, part I: Structure and circulation, *J. Appl. Meteorol.*, *36*, 1577–1598, 1997.

Camberlin, P., and O. Planchon, Coastal precipitation regimes in Kenya, *Geogr. Ann., Ser. A*, *79A*(1–2), 109–119, 1997.

Carbone, R. E., J. W. Wilson, T. D. Keenan, and J. M. Hacker, Tropical island convection is the absence of significant topography. part I: Life cycle of diurnally forced convection, *Mon. Weather Rev.*, *128*, 3459–3480, 2000.

Cenedese, A., M. Miozzi, and P. Monti, A laboratory investigation of land and sea breeze regimes, *Exp. Fluids*, suppl., S291–S299, 2000.

Chiba, O., The turbulent characteristics in the lowest part of the sea breeze front in the atmospheric surface layer, *Boundary Layer Meteorol.*, *65*, 181–195, 1993.

Chiba, O., F. Kobayashi, G. Naito, and K. Sassa, Helicopter observations of the sea breeze over a coastal area, *J. Appl. Meteorol.*, *38*, 481–492, 1999.

Clappier, A., A. Martilli, P. Grossi, P. Thunis, F. Pasi, B. C. Krueger, B. Calpini, G. Graziani, and H. van den Bergh, Effect of sea breeze on air pollution in greater Athens area, part I: Numerical simulations and field observations, *J. Appl. Meteorol.*, *39*, 546–562, 2000.

Clarke, R. H., Some observations and comments on the sea breeze, *Aust. Meteorol. Mag.*, *11*, 47–68, 1955.

Clarke, R. H., Colliding sea-breezes and the creation of internal atmospheric bore waves: Two-dimensional numerical studies, *Aust. Meteorol. Mag.*, *32*, 207–226, 1984.

Coutant, V., and V. L. Eichenlaub, *Theophrastus De Ventis*, 105 pp., Univ. of Notre Dame Press, Notre Dame, Ind., 1975.

Craig, R. A., I. Katz, and P. J. Harney, Sea breeze cross sections from pyschrometric measurements, *Bull. Am. Meteorol. Soc.*, *26*(10), 405–410, 1945.

Dalu, G. A., and R. A. Pielke, An analytical study of the sea breeze, *J. Atmos. Sci.*, *46*, 1815–1825, 1989.

Druilhet, A., A. Herrada, J. P. Pages, J. Saïssac, C. Allet, and M. Ravaut, Étude expérimentale de la couche limite interne associée à la brise de mer, *Boundary Layer Meteorol.*, *22*, 511–524, 1982.

Elliott, D. L., and J. J. O'Brien, Observational studies of the marine boundary layer over an upwelling region, *Mon. Weather Rev.*, *105*, 86–98, 1977.

Estoque, M. A., The sea breeze as a function of the prevailing synoptic situation, *J. Atmos. Sci.*, *19*, 244–250, 1962.

Federovich, E., F. T. M. Nieuwstadt, and R. Kaiser, Numerical and laboratory studies of horizontally evolving convective boundary layer, part II: Effects of elevated wind shear and surface roughness, *J. Atmos. Sci.*, *58*, 546–560, 2001.

Feliks, Y., A numerical model for estimation of the diurnal fluctuation of the inversion height due to a sea breeze, *Boundary Layer Meteorol.*, *62*, 151–161, 1993.

Finkele, K., Inland and offshore propagation speeds of a sea breeze from simulations and measurements, *Boundary Layer Meteorol.*, *87*, 307–329, 1998.

Finkele, K., J. M. Hacker, H. Kraus, and R. A. D. Byron-Scott, A complete sea-breeze circulation cell derived from aircraft observations, *Boundary Layer Meteorol.*, *73*, 299–317, 1995.

Fisher, E. L., An observational study of the sea breeze, *J. Meteorol.*, *17*, 645–660, 1960.

Franchito, S. H., V. B. Rao, J. L. Stech, and J. A. Lorenzzetti, The effect of coastal upwelling on the sea-breeze circulation of Cabo Frio, Brazil: A numerical experiment, *Ann. Geophys.*, *16*, 866–881, 1998.

Frizzola, J. A., and E. L. Fisher, A series of sea breeze observations in the New York City area, *J. Appl. Meteorol.*, *2*, 722–739, 1963.

Gangoiti, G., L. Alonso, M. Navazo, A. Albizuri, G. Perez-Landa, M. Matabuena, V. Valdenebro, M. Maruri, J. A. Garcia, and M. A. Millán, Regional transport of pollutants over the Bay of Biscay: Analysis of an ozone episode under a blocking anticyclone in west-central Europe, *Atmos. Environ.*, *36*, 1349–1361, 2002.

Garratt, J. R., and W. L. Physick, The inland boundary layer at low latitudes: II, Sea-breeze influences, *Boundary Layer Meteorol.*, *33*, 209–231, 1985.

Gaza, R. S., Mesoscale meteorology and high ozone in the northeast United States, *J. Appl. Meteorol.*, *37*, 961–977, 1998.

Geisler, J. E., and F. P. Bretherton, The sea-breeze forerunner, *J. Atmos. Sci.*, *26*, 82–95, 1969.

Gibbs, M. T., Detecting a response to weak sea breezes in the New South Wales coastal ocean, *N. Z. J. Mar. Freshwater Res.*, *34*, 669–680, 2000.

Godske, C. L., T. Bergeron, J. Bjerknes, and R. C. Bundgaard, *Dynamic Meteorology and Weather Forecasting*, 800 pp., Am. Meteorol. Soc., Boston, Mass., 1957.

Gryning, S. E., and E. Batchvarova, Analytical model for the growth of the coastal internal boundary layer during onshore flow, *Q. J. R. Meteorol. Soc.*, *116*, 187–203, 1990.

Hadi, T. W., T. Horinouchi, T. Tsuda, H. Hashiguchi, and S. Fuhao, Sea-breeze circulation over Jakarta, Indonesia: A climatology based on boundary layer radar observations, *Mon. Weather Rev.*, *130*, 2153–2166, 2002.

Halliday, D., R. Resnick, and J. Walker, *Fundamentals of Physics*, 1306 pp., John Wiley, Hoboken, N. J., 1993.

Helmis, C. G., D. N. Asimakopoulos, D. G. Deligiorgi, and D. P. Lalas, Observations of sea-breeze fronts near the shoreline, *Boundary Layer Meteorol.*, *38*, 395–410, 1987.

Helmis, C. G., K. H. Papadopoulos, J. A. Kalogiros, A. T. Soilemes, and D. N. Asimakopoulos, Influence of background flow on evolution of Saronic Gulf sea breeze, *Atmos. Environ.*, *29*, 3689–3701, 1995.

Holmer, B., and M. Haeger-Eugensson, Winter land breeze in a high latitude complex coastal area, *Phys. Geogr.*, *20*(2), 152–172, 1999.

Holton, J. R., *An Introduction to Dynamic Meteorology*, 511 pp., Academic, San Diego, Calif., 1992.

Hsu, S. A., *Coastal Meteorology*, 260 pp., Academic, San Diego, Calif., 1988.

Intrieri, J. M., C. G. Little, W. J. Shaw, R. M. Banta, P. A. Durkee, and R. M. Hardesty, The Land/Sea Breeze Experiment (LASBEX), *Bull. Am. Meteorol. Soc.*, *71*(5), 656–664, 1990.

Jehn, K. H., *A Sea Breeze Bibliography, 1664–1972, Rep. 37*, 51 pp., Atmos. Sci. Group, Coll. of Eng., Univ. of Tex., Austin 1973.

Kalthoff, N., et al., Mesoscale wind regimes in Chile at 30°S, *J. Appl. Meteorol.*, *41*, 953–970, 2002.

Kanda, M., Y. Inoue, and I. Uno, Numerical study on cloud lines over an urban street in Tokyo, *Boundary Layer Meteorol.*, *98*, 251–273, 2001.

Kitada, T., Turbulence structure of sea breeze front and its implication in air pollution transport—Application of k-e turbulence model, *Boundary Layer Meteorol.*, *41*, 217–239, 1987.

Kottmeier, C., P. Palacio-Sese, N. Kalthoff, U. Corsmeier, and F. Fiedler, Sea breezes and coastal jets in southeastern Spain, *Int. J. Climatol.*, *20*, 1791–1808, 2000.

Kozo, T. L., An observational study of sea breezes along the Alaskan Beaufort sea coast: Part I, *J. Appl. Meteorol.*, *21*, 891–905, 1982.

Kraus, H., Turbulence frontogenesis, *Meteorol. Atmos. Phys.*, *48*, 309–315, 1992.

Kraus, H., J. M. Hacker, and J. Hartmann, An observational aircraft-based study of sea-breeze frontogenesis, *Boundary Layer Meteorol.*, *53*, 223–265, 1990.

Kuelegan, G. H., An experimental study of the motion of saline water from locks into fresh water channels, in *13th Progress Report on Model Laws for Density Currents*, *Rep.*

5168, Natl. Inst. of Stand. and Technol., Gaithersburg, Md., 1957.

Laird, N. F., and D. A. R. Kristovich, Lake Michigan lake breezes: Climatology, local forcing, and synoptic environment, *J. Appl. Meteorol.*, *40*, 409–424, 2001.

Lapworth, A., Observations of atmospheric density currents using a tethered balloon-borne turbulence probe system, *Q. J. R. Meteorol. Soc.*, *126*, 2811–2850, 2000.

Lee, H. D. P., *Aristotle VII Meteorologica*, 432 pp., Harvard Univ. Press, Cambridge, Mass., 1952.

Lericos, T. P., H. E. Fuelberg, A. I. Watson, and R. L. Holle, Warm season lightning distributions over the Florida peninsula as related to synoptic patterns, *Weather Forecast.*, *17*, 83–98, 2002.

List, R. J., *Smithsonian Meteorological Tables*, 527 pp., Smithsonian Inst. Press, Washington, D. C., 1968.

Liu, H. P., and J. C. L. Chan, Boundary layer dynamics associated with a severe air-pollution episode in Hong Kong, *Atmos. Environ.*, *36*, 2013–2025, 2002.

Luhar, A. K., B. L. Sawford, J. M. Hacker, and K. N. Rayner, The Kwinana coastal fumigation study: II—Growth of the thermal internal boundary layer, *Boundary Layer Meteorol.*, *89*, 385–405, 1998.

Lutgens, F. K., and E. J. Tarbuck, *The Atmosphere an Introduction to Meteorology*, 484 pp., Prentice-Hall, Old Tappan, N. J., 2001.

Lyons, W. A., The climatology and prediction of the Chicago lake breeze, *J. Appl. Meteorol.*, *11*, 1259–1270, 1972.

Lyons, W. A., E. R. Sawdey, J. A. Schuh, R. H. Calby, and C. S. Keen, An updated and expanded coastal fumigation model, paper presented at 74th Annual Meeting, Air Pollut. Control Assoc., Philadelphia, Pa., 21–26 June 1981.

Masselink, G., and C. B. Pattiaratchi, The effect of sea breeze on beach morphology, surf zone hydrodynamics and sediment resuspension, *Mar. Geol.*, *146*, 115–135, 1998.

Mathews, J. H., The sea-breeze—Forecasting aspects, *Aust. Meteorol. Mag.*, *30*, 205–209, 1982.

McKendry, I., and N. Roulet, Sea breezes and advective effects in southwest James Bay, *J. Geophys. Res.*, *99*(D1), 1623–1634, 1994.

McPherson, R. D., A numerical study of the effect of a coastal irregularity on the sea breeze, *J. Appl. Meteorol.*, *9*, 767–777, 1970.

Melas, D., and H. D. Kambezidis, The depth of the internal boundary layer over an urban area under sea-breeze conditions, *Boundary Layer Meteorol.*, *61*, 247–264, 1992.

Melas, D., I. Ziomas, O. Klemm, and C. S. Zerefos, Anatomy of the sea-breeze circulation in Athens area under weak large-scale ambient winds, *Atmos. Environ.*, *32*, 2223–2237, 1998.

Melas, D., A. Lavagnini, and A. Sempreviva, An investigation of the boundary layer dynamics of Sardinia Island under sea-breeze conditions, *J. Appl. Meteorol.*, *39*, 516–524, 2000.

Miller, J. E., On the concept of frontogenesis, *J. Meteorol.*, *5*, 169–171, 1948.

Miller, S. T. K., and B. D. Keim, Synoptic-scale controls on the sea breeze of the central New England coast, *Weather Forecast.*, *18*, 236–248, 2003.

Mitsumoto, S., H. Ueda, and H. Ozoe, A laboratory experiment on the dynamics of the land and sea breezes, *J. Atmos. Sci.*, *40*, 1228–1240, 1983.

Mizuma, M., General aspects of land and sea breezes in Osaka Bay and surrounding area, *J. Meteorol. Soc. Jpn.*, *73*(6), 1029–1040, 1995.

Mizuma, M., General aspects of land and sea breezes in western Seto Inland Sea and surrounding areas, *J. Meteorol. Soc. Jpn*, *76*(3), 403–418, 1998.

Neumann, J., On the rotation rate of the direction of sea and land breezes, *J. Atmos. Sci.*, *34*, 1913–1917, 1977.

Neumann, J., and Y. Mahrer, A theoretical study of the land and sea breeze circulation, *J. Atmos. Sci.*, *28*, 532–542, 1971.

Nielsen., J. W., In situ observations of Kelvin-Helmholtz waves along a frontal inversion, *J. Atmos. Sci.*, *49*, 369–386, 1992.

Ohashi, Y., and H. Kida, Observational results of the sea breeze with a weak wind region over the northern Osaka urban area, *J. Meteorol. Soc. Jpn.*, *79*(4), 949–955, 2002.

Oliphant, A. J., A. P. Sturman, and N. J. Tapper, The evolution and structure of a tropical island sea/land-breeze system, northern Australia, *Meteorol. Atmos. Phys.*, *78*, 45–59, 2001.

Pagnotti, V., A meso-meteorological feature associated with high ozone concentrations in the northeastern United States, *JAPCA*, *37*(6), 720–722, 1987.

Panel on Coastal Meteorology, *Coastal Meteorology—A Review of the State of the Science*, 99 pp., Natl. Acad. Press, Washington, D. C., 1992.

Pearce, R. P., The calculation of a sea-breeze circulation in terms of differential heating across the coastline, *Q. J. R. Meteorol. Soc.*, *81*, 351–381, 1955.

Pearson, R. A., G. Carboni, and G. Brusasca, The sea breeze with mean flow, *Q. J. R. Meteorol. Soc.*, *109*, 809–830, 1983.

Physick, W. L., Numerical experiments on the inland penetration of the sea breeze, *Q. J. R. Meteorol. Soc.*, *106*, 735–746, 1980.

Physick, W. L., and D. J. Abbs, Flow and plume dispersion in a coastal valley, *J. Appl. Meteorol.*, *31*, 64–73, 1992.

Pielke, R. A., Sea breeze-induced mesoscale systems and severe weather, *NASA Proj. Prog. Rep. NASA-CR-174317*, NASA, Greenbelt, Md., 1985.

Pielke, R. A., A. Song, P. J. Michaels, W. A. Lyons, and R. W. Arritt, The predictability of sea-breeze generated thunderstorms, *Atmosfera*, *4*, 65–78, 1991.

Planchon, O., and S. Cautenet, Rainfall and sea-breeze circulation over south-western France, *Int. J. Climatol.*, *17*, 535–549, 1997.

Prahba, T. V., R. Venkatesan, E. Mursch-Radlgruber, G. Rengarajan, and N. Jayanthi, Thermal internal boundary layer characteristics at a tropical coastal site as observed by a mini-SODAR under varying synoptic conditions, *Proc. Indian Acad. Sci. Earth Planet Sci.*, *111*(1), 63–77, 2002.

Rao, P., and H. E. Fuelberg, An investigation of convection behind the Cape Canaveral sea-breeze front, *Mon. Weather Rev.*, *128*, 3437–3458, 2000.

Raynor, G. S., S. Sethuraman, and R. M. Brown, Formation and characteristics of coastal internal boundary layers during onshore flows, *Boundary Layer Meteorol.*, *16*, 487–514, 1979.

Reible, D. D., J. E. Simpson, and P. F. Linden, The sea breeze and gravity-current frontogenesis, *Q. J. R. Meteorol. Soc.*, *119*, 1–16, 1993.

Rogers, R. R., and M. K. Yau, *A Short Course in Cloud Physics*, 290 pp., Butterworth-Heinemann, Woburn, Mass., 1989.

Rotunno, R., On the linear theory of the land and sea breeze, *J. Atmos. Sci.*, *40*, 1999–2009, 1983.

Rubes, M. T., H. J. Cooper, and E. A. Smith, A study of the Merritt Island, Florida sea breeze flow regimes and their effect on surface heat and moisture fluxes, *NASA Contract. Rep. 4537*, 141 pp., NASA, Greenbelt, Md., 1993.

Sawford, B. L., A. K. Luhar, J. H. Hacker, S. A. Young, I.-H. Yoon, J. A. Noonan, J. N. Carras, D. J. Williams, and K. N. Rayner, The Kwinana coastal fumigation study: I—Program overview, experimental design, and selected results, *Boundary Layer Meteorol.*, *89*, 359–384, 1998.

Schoellhamer, D. H., Factors affecting suspended-solids concentrations in south San Francisco Bay, California, *J. Geophy. Res.*, *101*(C5), 12,087–12,095, 1996.

Schoenberger, L. M., Doppler radar observation of a land-breeze cold front, *Mon. Weather Rev.*, *112*, 2455–2464, 1984.

Schumann, E. H., W. K. Illenberger, and W. S. Goschen,

Surface winds over Algoa Bay, South Africa, *S. Afr. J. Sci.*, *87*, 202–207, 1991.
Seaman, N. L., and S. A. Michelson, Mesoscale meteorological structure of a high-ozone episode during the 1995 NARSTO-Northeast Study, *J. Appl. Meteorol.*, *39*, 384–398, 2000.
Sha, W., T. Kawamura, and H. Ueda, A numerical study on sea-land breezes as a gravity current: Kelvin-Helmholtz billows and inland penetration of the sea-breeze front, *J. Atmos. Sci.*, *48*, 1649–1665, 1991.
Sha, W., T. Kawamura, and H. Ueda, A numerical study of nocturnal sea breezes: Prefrontal gravity waves in the compensating flow and inland penetration of the sea-breeze cutoff vortex, *J. Atmos. Sci.*, *50*, 1076–1087, 1993.
Shair, F. H., E. J. Sasaki, D. E. Carlan, G. R. Cass, W. R. Goodin, J. G. Edinger, and G. E. Schacher, Transport and dispersion of airborne pollutants associated with the land breeze-sea breeze system, *Atmos. Environ.*, *16*, 2043–2053, 1982.
Shearer, D. L., and R. J. Kaleel, Critical review of studies on atmospheric dispersion in coastal regions, *Rep. PNL-4292*, 41 pp., Pac. Natl. Lab., Richland, Wash., 1982.
Silva Dias, M. A. F., and A. J. Machado, The role of local circulations in summertime convective development and nocturnal fog in São Paulo, Brazil, *Boundary Layer Meteorol.*, *82*, 135–157, 1997.
Simpson, J. E., A comparison between laboratory currents and atmospheric density currents, *Q. J. R. Meteorol. Soc.*, *95*, 758–765, 1969.
Simpson, J. E., *Sea Breeze and Local Wind*, 234 pp., Cambridge Univ. Press, New York, 1994.
Simpson, J. E., Diurnal changes in sea-breeze direction, *J. Appl. Meteorol.*, *35*, 1166–1169, 1996.
Simpson, J. E., *Gravity Currents in the Environment and the Laboratory*, 244 pp., Cambridge Univ. Press, New York, 1997.
Simpson, J. E., and R. E. Britter, A laboratory model of an atmospheric mesofront, *Q. J. R. Meteorol. Soc.*, *106*, 485–500, 1980.
Simpson, J. E., D. A. Mansfield, and J. R. Milford, Inland penetration of sea-breeze fronts, *Q. J. R. Meteorol. Soc.*, *103*, 47–76, 1977.
Smith, R. K., N. Crook, and G. Roff, The Morning Glory: An extraordinary atmospheric undular bore, *Q. J. R. Meteorol. Soc.*, *108*, 937–956, 1982.
Stephan, K., H. Kraus, C. M. Ewenz, and J. M. Hacker, Sea-breeze front variations in space and time, *Meteorol. Atmos. Phys.*, *70*, 81–95, 1999.
Stull, R. B., *An Introduction to Boundary Layer Meteorology*, 670 pp., Kluwer Acad., Norwell, Mass., 1988.
Tijm, A. B. C., and A. J. van Delden, The role of sound waves in sea-breeze circulation, *Q. J. R. Meteorol. Soc.*, *125*, 1997–2018, 1999.
Tijm, A. B. C., A. A. M. Holtstag, and A. J. van Delden, Observations and modeling of the sea breeze with the return current, *Mon. Weather Rev.*, *127*, 625–640, 1999.
Venkatram, A., A model of internal boundary-layer development, *Boundary Layer Meteorol.*, *11*, 419–437, 1977.
Walsh, J. E., Sea breeze theory and applications, *J. Atmos. Sci.*, *31*, 2012–2026, 1974.
Weckwerth, T. M., J. W. Wilson, and R. M. Wakimoto, Thermodynamic variability within the convective boundary layer due to horizontal convective rolls, *Mon. Weather Rev.*, *124*, 769–784, 1996.
Weckwerth, T. M., J. W. Wilson, R. M. Wakimoto, and N. A. Crook, Horizontal convective rolls: Determining the environmental conditions supporting their existence and characteristics, *Mon. Weather Rev.*, *125*, 505–526, 1997.
Wood, R., I. M. Stromberg, and P. R. Jonas, Aircraft observations of sea-breeze frontal structure, *Q. J. R. Meteorol. Soc.*, *125*, 1959 –1995, 1999.
Xian, Z., and R. A. Pielke, The effects of width of landmasses on the development of sea breezes, *J. Appl. Meteorol.*, *30*, 1280–1304, 1991.
Xu, Q., Density currents in shear flows—A two-fluid model, *J. Atmos. Sci.*, *49*, 511–524, 1992.
Yoshikado, H., Numerical study of the daytime urban effect and its interaction with the sea breeze, *J. Appl. Meteorol.*, *31*, 1146–1164, 1992.
Yu, T. W., and N. K. Wagner, Diurnal variations of onshore wind speed near a coastline, *J. Appl. Meteorol.*, *9*, 760–766, 1970.
Zhong, S., and E. S. Takle, An observational study of sea- and land-breeze circulation in an area of complex coastal heating, *J. Appl. Meteorol.*, *31*, 1426–1438, 1992.

B. D. Keim, Southern Regional Climate Center, Louisiana State University, Baton Rouge, LA 70803, USA. (bkeim@srcc.lsu.edu)

H. Mao, S. T. K. Miller, and R. W. Talbot, Climate Change Research Center, Institute for the Study of Earth, Oceans and Space, University of New Hampshire, Durham, NH 03824, USA. (hmao@typhoon.sr.unh.edu; stm@cisunix.unh.edu; bob@resolution.sr.unh.edu)